IMA Journal of Numerical Analysis (2020) **40**, 886–913
doi:10.1093/imanum/dry094
Advance Access publication on 25 January 2019

A Leray regularized ensemble-proper orthogonal decomposition method for parameterized convection-dominated flows

Max Gunzburger
Department of Scientific Computing, Florida State University, Tallahassee, FL 32306-4120, USA
mgunzburger@fsu.edu

Traian Iliescu
Department of Mathematics, Virginia Tech, Blacksburg, VA 24061-0123, USA
iliescu@vt.edu

and

Michael Schneier*
Department of Scientific Computing, Florida State University, Tallahassee, FL 32306-4120, USA
*Corresponding author: mhs13c@my.fsu.edu

[Received on 16 November 2017; revised on 16 September 2018]

Partial differential equations (PDEs) are often dependent on input quantities that are uncertain. To quantify this uncertainty PDEs must be solved over a large ensemble of parameters. Even for a single realization this can be a computationally intensive process. In the case of flows governed by the Navier–Stokes equations, an efficient method has been devised for computing an ensemble of solutions. To further reduce the computational cost of this method, an ensemble-proper orthogonal decomposition (POD) method was recently proposed. The main contribution of this work is the introduction of POD spatial filtering for ensemble-POD methods. The POD spatial filter makes possible the construction of the Leray ensemble-POD model, which is a regularized-reduced order model for the numerical simulation of convection-dominated flows of moderate Reynolds number. The Leray ensemble-POD model employs the POD spatial filter to smooth (regularize) the convection term in the Navier–Stokes equations, and diminishes the numerical inaccuracies produced by the ensemble-POD method in the numerical simulation of convection-dominated flows. Specifically, for the numerical simulation of a convection-dominated two-dimensional flow between two offset cylinders, we show that the Leray ensemble-POD method better reflects the dynamics of the benchmark results than the ensemble-POD scheme. The second contribution of this work is a new numerical discretization of the variable viscosity ensemble algorithm in which the average viscosity is replaced with the maximum viscosity. It is shown that this new numerical discretization is significantly more stable than those in current use. Furthermore, error estimates for the novel Leray ensemble-POD algorithm with this new numerical discretization are also proven.

Keywords: Navier–Stokes equations; ensemble computation; proper orthogonal decomposition; Leray regularization; POD differential filter.

1. Introduction

Mathematical flow models inherently rely on fundamental input quantities whose actual values are imperfectly measured or sensitive to variations in other parameters. These quantities include the initial

conditions, forcing functions and model coefficients. In order to develop robust models, the impact of this uncertainty must be quantified. Robust flow models must identify and properly handle parameter influence whose sensitivity or uncertainty affects model behavior. Such robust flow models are vitally important for numerical weather forecasting, ocean modeling, aeronautical design and hemodynamics. For example, the commonly used 'spaghetti plot' (which displays different possibilities of a hurricane's path subject to uncertainties in the initial conditions) will tighten its predicted spread, directly leading to more timely evacuation plans.

Common approaches for recovering accurate solution statistics of these models are the Monte Carlo and stochastic collocation methods (Ganapathysubramanian & Zabaras, 2007; Nobile *et al.*, 2008a,b; Chkifa *et al.*, 2014, 2015; Gunzburger *et al.*, 2014). These algorithms all require the underlying model to be solved over an ensemble of parameters. Depending upon the problem, the spatial resolution required for accurate realizations of the model can render these approaches computationally intractable. In particular, realizations for flow models such as the incompressible Navier–Stokes equations (NSEs) can take on the order of weeks. In this work we are interested in computing ensembles of solutions for the NSE with uncertainty present in the initial conditions, viscosities and body forces. Specifically, for $j = 1, \ldots, J$, we have

$$\begin{cases} u_t^j + u^j \cdot \nabla u^j - \nu_j \Delta u^j + \nabla p^j = f^j(x,t) & \forall x \in \Omega \times (0,T] \\ \nabla \cdot u^j = 0 & \forall x \in \Omega \times (0,T] \\ u^j = 0 & \forall x \in \partial\Omega \times (0,T] \\ u^j(x,0) = u^{j,0}(x) & \forall x \in \Omega, \end{cases} \tag{1.1}$$

where $\Omega \subset \mathbb{R}^d$, $d = 2, 3$, is an open regular domain. We note that the case where viscosity depends on space or time is not considered. This would reflect fluid inhomogeneities; one potential cause of this could be due to slight temperature variations. First steps towards analyzing this form of the problem in the ensemble framework have been taken in Anthony (2018).

If we consider a standard spatial and time discretization of problem (1.1) this results in the need to solve J different linear systems at each time step (i.e., a separate linear system for each parameter). Depending on the number of parameters J and the spatial resolution, an infeasible amount of computational resources may be necessary to solve these separate problems. Recently, new algorithms have been developed to overcome this computational barrier (Jiang, 2014, 2017; Jiang & Layton, 2014; Takhirov *et al.*, 2016; Luo & Wang, 2017; Mohebujjaman & Rebholz, 2017) that allow for simultaneous calculations at each time step. Specifically, the focus of these algorithms has been to use the same linear system for each right-hand side. Taking advantage of this problem structure efficient block solvers, such as block conjugate gradient (Feng *et al.*, 1995), block quasi-minimal residual (Freund & Malhotra, 1997) and block generalized minimal residual (Gallopulos & Simoncini, 1996), can then be utilized.

To further improve the efficiency of these ensemble algorithms reduced-order models (ROMs) (Hesthaven *et al.*, 2015; Quarteroni *et al.*, 2015) were recently utilized (Gunzburger *et al.*, 2017, 2018). Specifically, the proper orthogonal decomposition (POD) method was used to extract the dominant (most energetic) modes from a high-resolution numerical simulation, and the NSEs were projected onto these POD modes to obtain an ensemble-POD model. In Gunzburger *et al.* (2017, 2018) it was shown that the ensemble-POD model significantly decreased the computational cost of the standard ensemble methods, without compromising their numerical accuracy. We note, however, that the numerical investigation of the ensemble-POD model in Gunzburger *et al.* (2017, 2018) was restricted to low Reynolds numbers. It is well known that, for convection-dominated flows, standard

ROMs generally yield inaccurate results, usually in the form of spurious numerical oscillations (see, e.g., Giere *et al.* (2015); Xie *et al.* (2017a,b)). To mitigate these ROM inaccuracies, several numerical stabilization techniques have been proposed over the years (see, e.g., Weller *et al.* (2009a,b); Kalashnikova & Barone (2010); Carlberg *et al.* (2013); Balajewicz *et al.* (2013, 2016); Östh *et al.* (2014); Benosman *et al.* (2016); Wang *et al.* (2016); Chacón Rebollo *et al.* (2017); Fick *et al.* (2017)). Regularized ROMs (Reg-ROMs) are recently proposed stabilized ROMs for the numerical simulation of convection-dominated flows, both deterministic (Sabetghadam & Jafarpour, 2012; Wells *et al.*, 2017; Xie *et al.*, 2018) and stochastic (Iliescu *et al.*, 2018). These Reg-ROMs use explicit ROM spatial filtering to regularize (smooth) various ROM terms and thus increase the numerical stability of the resulting ROM. This idea was first used by Leray (1934) in the mathematical study of the NSE and later on in, e.g., Geurts & Holm (2003) and Layton & Rebholz (2012) to develop regularized models for the numerical simulation of turbulent flows (Geurts & Holm, 2003; Layton & Rebholz, 2012). In the ROM arena Reg-ROMs were also successfully used in the numerical simulation of convection-dominated flows. For example, the Reg-ROMs used in the numerical simulation of a three-dimensional flow past a circular cylinder at a Reynolds number $Re = 1000$ produced accurate results in which the spurious numerical oscillations of standard ROMs were significantly decreased (Wells *et al.*, 2017).

In this paper we put forth ROM spatial filtering and Reg-ROMs as a means to mitigate the numerical inaccuracies that are generally produced by the ensemble-POD method when this is applied to convection-dominated flows of moderate Reynolds number. Specifically, we propose and investigate the Leray ensemble-POD method, which replaces the convective field in the nonlinearity of the standard ensemble-POD method with its spatially filtered version. For the spatial filter in the Leray ensemble-POD method we use the POD differential filter (Wells *et al.*, 2017; Xie *et al.*, 2017b). In Section 3 we also propose a new numerical discretization of the variable viscosity ensemble algorithm in which the average viscosity is replaced with the maximum viscosity. The idea of using the maximum viscosity comes from the algorithms presented in Johnston & Liu (2004) and Anitescu *et al.* (2004). We show that this new numerical discretization is significantly more stable than those in current use. Furthermore, we prove error estimates for the new Leray ensemble-POD algorithm with this new numerical discretization. Finally, in Section 6, we test the new Leray ensemble-POD method in the numerical simulation of the two-dimensional flow between offset circles used in Gunzburger *et al.* (2017, 2018). To this end we compare the new Leray ensemble-POD method with the standard ensemble-POD method and a fine resolution numerical simulation, which is used as a benchmark.

2. Notation and preliminaries

We denote by $\|\cdot\|$ and $(\cdot,\cdot)$ the $L^2(\Omega)$ norm and inner product, respectively, and by $\|\cdot\|_{L^p}$ and $\|\cdot\|_{W_p^k}$ the $L^p(\Omega)$ and Sobolev $W_p^k(\Omega)$ norms, respectively. $H^k(\Omega) = W_2^k(\Omega)$ with norm $\|\cdot\|_k$. For a function $v(x,t)$ that is well defined on $\Omega \times [0,T]$ we define the norms

$$|||v|||_{2,s} := \left(\int_0^T \|v(\cdot,t)\|_s^2 \, \mathrm{d}t\right)^{\frac{1}{2}} \qquad \text{and} \qquad |||v|||_{\infty,s} := \operatorname{ess\,sup}_{[0,T]} \|v(\cdot,t)\|_s.$$

The space $H^{-1}(\Omega)$ denotes the dual space of bounded linear functionals defined on $H_0^1(\Omega) = \{v \in H^1(\Omega) \,:\, v = 0 \text{ on } \partial\Omega\}$; this space is equipped with the norm

$$\|f\|_{-1} = \sup_{0 \neq v \in X} \frac{(f,v)}{\|\nabla v\|} \quad \forall f \in H^{-1}(\Omega).$$

The solutions spaces X for the velocity and Q for the pressure are respectively defined as

$$X := [H_0^1(\Omega)]^d = \{v \in [L^2(\Omega)]^d \,:\, \nabla v \in [L^2(\Omega)]^{d\times d} \text{ and } v = 0 \text{ on } \partial\Omega\}$$
$$Q := L_0^2(\Omega) = \left\{q \in L^2(\Omega) \,:\, \int_\Omega q \,\mathrm{d}x = 0\right\}.$$

A weak formulation of (1.1) is given as follows: for $j = 1, \ldots, J$, find $u^j : (0, T] \to X$ and $p^j : (0, T] \to Q$ such that, for almost all $t \in (0, T]$, satisfy

$$\begin{cases} (u_t^j, v) + (u^j \cdot \nabla u^j, v) + \nu_j(\nabla u^j, \nabla v) - (p^j, \nabla \cdot v) = (f^j, v) & \forall\, v \in X \\ (\nabla \cdot u^j, q) = 0 & \forall\, q \in Q \\ u^j(x, 0) = u^{j,0}(x). \end{cases} \tag{2.1}$$

The subspace of X consisting of weakly divergence-free functions is defined as

$$V := \{v \in X \,:\, (\nabla \cdot v, q) = 0 \;\forall\, q \in Q\} \subset X.$$

We denote conforming velocity and pressure finite element spaces based on a regular triangulation of Ω having maximum triangle diameter h by $X_h \subset X$ and $Q_h \subset Q$. We assume that the pair of spaces (X_h, Q_h) satisfy the discrete inf-sup (or LBB_h) condition required for stability of finite element approximations; we also assume that the finite element spaces satisfy the approximation properties

$$\inf_{v_h \in X_h} \|v - v_h\| \leqslant Ch^{s+1} \quad \forall\, v \in [H^{s+1}(\Omega)]^d$$
$$\inf_{v_h \in X_h} \|\nabla(v - v_h)\| \leqslant Ch^{s} \quad \forall\, v \in [H^{s+1}(\Omega)]^d$$
$$\inf_{q_h \in Q_h} \|q - q_h\| \leqslant Ch^{s} \quad \forall\, q \in H^{s}(\Omega),$$

where C is a positive constant that is independent of h. The Taylor–Hood element pairs (P^s-P^{s-1}), $s \geqslant 2$, are one common choice for which the LBB_h stability condition and the approximation estimates hold (Girault & Raviart, 1979; Gunzburger, 2012).

To ensure the uniqueness of the NSE solution and ensure that standard finite element error estimates hold, we make the following regularity assumptions on the data and true solution.

Assumption 2.1 In (1.1) we assume that $u^0 \in V$, $f^j \in L^2(0, T; L^2(\Omega))$, $u^j \in L^\infty(0, T; H^{s+1}(\Omega)) \cap H^1(0, T; H^{s+1}(\Omega)) \cap H^2(0, T; L^2(\Omega))$ and $p \in L^\infty(0, T; Q \cap H^k(\Omega))$.

Using the above regularity assumptions and assuming a sufficiently small Δt, the following error estimate can be proven for the full discretization of (2.1) with Taylor–Hood elements and the Crank–Nicolson time-discretization (Layton *et al.*, 2008; John *et al.*, 2016):

$$\|u^j(t^N) - u_h^{j,N}\|^2 + \nu\, \Delta t \sum_{n=1}^{M} \|\nabla(u^j(t^n) - u_h^{j,n})\|^2 \leqslant C\left(h^{2m} + \Delta t^4\right), \tag{2.2}$$

where C is independent of h and Δt.

We define the trilinear form

$$b(w,u,v) = (w\cdot\nabla u, v) \qquad \forall u,v,w \in [H^1(\Omega)]^d$$

and the explicitly skew-symmetric trilinear form given by

$$b^*(w,u,v) := \frac{1}{2}(w\cdot\nabla u, v) - \frac{1}{2}(w\cdot\nabla v, u) \qquad \forall u,v,w \in [H^1(\Omega)]^d,$$

which satisfies the bounds (Layton, 2008)

$$b^*(w,u,v) \leqslant C_{b^*}\|\nabla w\|\|\nabla u\|(\|v\|\|\nabla v\|)^{1/2} \qquad \forall\, u,v,w \in X \tag{2.3}$$

$$b^*(w,u,v) \leqslant C_{b^*}(\|w\|\|\nabla w\|)^{1/2}\|\nabla u\|\|\nabla v\| \qquad \forall\, u,v,w \in X. \tag{2.4}$$

We also define the discretely divergence-free space V_h as

$$V_h := \{v_h \in X_h \,:\, (\nabla\cdot v_h, q_h) = 0\ \forall\, q_h \in Q_h\} \subset X.$$

In most cases, and for the Taylor–Hood element pair in particular, $V_h \not\subset V$, i.e., discretely divergence-free functions are not weakly divergence-free.

DEFINITION 2.2 Let $t^n = n\Delta t$, $n = 0,1,2,\ldots,N$, where $N := T/\Delta t$, denote a partition of the interval $[0,T]$. For $j = 1,\ldots,J$ and $n = 0,1,2,\ldots,N$ let $u^{j,n}(x) := u^j(x,t^n)$. Then the **ensemble mean** is defined, for $n = 0,1,2,\ldots,N$, by

$$< u >^n := \frac{1}{J}\sum_{j=1}^{J} u^{j,n}.$$

The full space and time model on which we base our method is similar to the one used in Gunzburger *et al.* (2017a,b). For $j = 1,\ldots,J$, given $u_h^{j,0} \in X_h$ and $u_h^{j,1} \in X_h$, for $n = 0,1,2,\ldots,N-1$ find $u_h^{j,n+1} \in X_h$ and $p_h^{j,n+1} \in Q_h$, satisfying

$$\begin{aligned}
&\left(\frac{u_h^{j,n+1} - u_h^{j,n}}{\Delta t}, v_h\right) + b^*(< u_h >^n, u_h^{j,n+1}, v_h) + b^*(u_h^{j,n} - < u_h >^n, u_h^{j,n}, v_h)\\
&\qquad + \nu_{max}(\nabla u_h^{j,n+1}, \nabla v_h) + (\nu_j - \nu_{max})(\nabla u_h^{j,n}, \nabla v_h)\\
&\qquad - (p_h^{j,n+1}, \nabla\cdot v_h) = (f^{j,n+1}, v_h) \quad \forall\, v_h \in X_h\\
&\qquad\qquad (\nabla\cdot u_h^{j,n+1}, q_h) = 0 \qquad \forall\, q_h \in Q_h.
\end{aligned} \tag{2.5}$$

The major difference between the two algorithms is the use of maximum value of the viscosities ν_{max} rather than the average $< \nu >$, resulting in a superior stability condition.

3. POD-ensemble–based models

3.1 *POD*

In this subsection we briefly describe the POD method and apply it to the previously stated ensemble algorithm. A more detailed description of this method can be found in Kunisch & Volkwein (2001).

Given a positive integer N_S let $0 = t_0 < t_1 < \cdots < t_{N_S} = T$ denote a uniform partition of the time interval $[0, T]$. For $j = 1, \ldots, J_S$ we select J_S different initial conditions $u^{j,0}(x)$, viscosities ν^j and forcing functions f^j and denote by $u_{h,S}^{j,m}(x) \in X_h$, $j = 1, \ldots, J_S$, $m = 1, \ldots, N_S$ the finite element approximation to (1.1) evaluated at $t = t_m$, $m = 1, \ldots, N_S$. We then define the space spanned by the $J_S(N_S + 1)$ discrete snapshots as

$$X_{h,S} := \operatorname{span}\{u_{h,S}^{j,m}(x)\}_{j=1,m=0}^{J_S,N_S} \subset V_h \subset X_h.$$

Denoting by $\vec{u}_S^{\,j,m}$ the vector of coefficients corresponding to the finite element function $u_{h,S}^{j,m}(x)$, where $K = \dim X_h$, we define the $K \times J_S(N_S + 1)$ *snapshot matrix* $\mathbb{A}$ as

$$\mathbb{A} = \left(\vec{u}_S^{\,1,0}, \vec{u}_S^{\,1,1}, \ldots, \vec{u}_S^{\,1,N_S}, \vec{u}_S^{\,2,0}, \vec{u}_S^{\,2,1}, \ldots, \vec{u}_S^{\,2,N_S}, \ldots, \vec{u}_S^{\,J_S,0}, \vec{u}_S^{\,J_S,1}, \ldots, \vec{u}_S^{\,J_S,N_S}\right),$$

i.e., the columns of $\mathbb{A}$ are the finite element coefficient vectors corresponding to the discrete snapshots. The POD method then seeks a low-dimensional basis

$$X_R := \operatorname{span}\{\varphi_i\}_{i=1}^{R} \subset X_{h,S} \subset V_h \subset X_h$$

that can approximate the snapshot data. This basis can be determined by solving the constrained minimization problem

$$\min \sum_{k=1}^{J_S} \sum_{l=0}^{N_S} \left\| u_{h,s}^{k,l} - \sum_{j=1}^{R} (u_{h,s}^{k,l}, \varphi_j)\varphi_j \right\|^2 \qquad \text{subject to} (\varphi_i, \varphi_j) = \delta_{ij} \quad \text{for } i, j = 1, \ldots, R, \tag{3.1}$$

where δ_{ij} denotes the Kronecker delta. Defining the correlation matrix $\mathbb{C} = \mathbb{A}^T \mathbb{M} \mathbb{A}$, where $\mathbb{M}$ denotes the finite element mass matrix, this problem can then be solved by considering the eigenvalue problem

$$\mathbb{C}\vec{a}_i = \lambda_i \vec{a}_i.$$

It can then be shown that the POD basis functions will be given by

$$\vec{\varphi}_i = \frac{1}{\sqrt{\lambda_i}} \mathbb{A}\vec{a}_i, \quad i = 1, \ldots, R.$$

We now define the POD L^2 projection that we need for the ensuing stability and error analysis.

DEFINITION 3.1 (POD L^2 projection). Let $P_r : L^2(\Omega) \to X_R$ such that

$$(u - P_r u, \varphi) = 0 \qquad \forall \varphi \in X_R. \tag{3.2}$$

Next we give a POD inverse estimate. Let $\mathbb{S}_R = (\nabla\varphi_i, \nabla\varphi_j)_{L^2}$ be the POD stiffness matrix and let $|||\cdot|||_2$ denote the matrix 2-norm.

LEMMA 3.2 (POD inverse estimate).

$$\|\nabla\varphi\| \leqslant |||\mathbb{S}_R|||_2^{\frac{1}{2}} \|\varphi\| \quad \forall\, \varphi \in X_R. \tag{3.3}$$

3.2 *Ensemble-POD algorithm*

Using this POD basis we can now construct the ensemble-POD algorithm. The construction is similar to the full finite element approximation, except we seek a solution in the POD space X_R using the basis $\{\varphi_i\}_{i=1}^R$. The fully discrete algorithm can be written as

$$\left(\frac{u_R^{j,n+1} - u_R^{j,n}}{\Delta t}, \varphi\right) + b^*(< u_R >^n, u_R^{j,n+1}, \varphi) + b^*(u_R^{j,n} - < u_R >^n, u_R^{j,n}, \varphi)$$
$$+ \nu_{max}(\nabla u_R^{j,n+1}, \nabla\varphi) + (\nu_j - \nu_{max})(\nabla u_R^{j,n}, \nabla\varphi) = (f^{j,n+1}, \varphi) \qquad \forall\, \varphi \in X_R. \tag{3.4}$$

We note that because $X_R \subset V_h$ the POD basis is discretely divergence-free by construction. Therefore, there is no pressure term present in (3.2). In recent works constructing a basis for the pressure space in addition to the velocity space has been investigated. The interested reader should consult Ballarin *et al.* (2015).

3.3 *Leray ensemble-POD algorithm*

To construct the Leray ensemble-POD algorithm we use the ROM differential filter.

DEFINITION 3.3 (ROM differential filter). $\forall v \in X$ let $\overline{v}^R$ be the unique element of X_R such that

$$\delta^2(\nabla\overline{v}^R, \nabla\varphi) + (\overline{v}^R, \varphi) = (v, \varphi) \qquad \forall\, \varphi \in X_R. \tag{3.5}$$

Here δ is known as the filtering radius. The differential filter was first developed by Germano (1986) for large eddy simulations. It was introduced in the ROM setting in Sabetghadam & Jafarpour (2012) and expanded further in Wells *et al.* (2017) and Xie *et al.* (2018).

Incorporating this into the ensemble framework, the fully discrete Leray ensemble-POD algorithm can be written as

$$\left(\frac{u_R^{j,n+1} - u_R^{j,n}}{\Delta t}, \varphi\right) + b^*(\overline{< u_R >^n}, u_R^{j,n+1}, \varphi) + b^*(\overline{u_R^{j,n} - < u_R >^n}, u_R^{j,n}, \varphi)$$
$$+ \nu_{max}(\nabla u_R^{j,n+1}, \nabla\varphi) + (\nu_j - \nu_{max})(\nabla u_R^{j,n}, \nabla\varphi) = (f^{j,n+1}, \varphi) \qquad \forall\, \varphi \in X_R. \tag{3.6}$$

4. Stability analysis

In this section we present a result pertaining to the stability of the Leray ensemble-POD algorithm. A stability bound for the ensemble-POD algorithm for a fixed viscosity was proven in Gunzburger *et al.* (2017, Theorem 4.2), while a stability bound for an ensemble-finite element algorithm with variable

viscosity was proven in Gunzburger *et al.* (2017b, Theorem 2.1). The stability bound proven in this section is less restrictive than the bound proven in Gunzburger *et al.* (2017b) due to the use of ν_{max} in the algorithm as opposed to $< \nu >$.

THEOREM 4.1 Consider algorithm (3.6); define $0 \leqslant \varepsilon \leqslant 1$ such that

$$\max_{1 \leqslant j \leqslant J} \frac{|\nu_j - \nu_{max}|}{\nu_{max}} = 1 - \varepsilon \tag{4.1}$$

and assume the following condition holds for $j = 1 \ldots J$:

$$\frac{C_{b^*}^2 \, \Delta t}{\nu_{max}} |||\mathbb{S}_R|||_2^{\frac{1}{2}} \|\nabla(\overline{u_R^{j,n} - < u_R >^n})\|^2 \leqslant \varepsilon. \tag{4.2}$$

Then for any $N1$

$$\begin{aligned} &\frac{1}{2}\|u_R^{j,N}\|^2 + \frac{\nu_{max}\Delta t}{2}\|\nabla u_R^{j,N}\|^2 + \frac{\varepsilon\, \nu_{max}\, \Delta t}{4}\sum_{n=0}^{N-1}\|u_R^{j,n+1}\|^2 \\ &\leqslant \sum_{n=0}^{N-1}\frac{\Delta t}{\nu_{max}\varepsilon}\|f_j^{n+1}\|_{-1}^2 + \frac{1}{2}\|u_R^0\|^2 + \frac{\nu_{max}\Delta t}{2}\|\nabla u_R^{j,0}\|^2 \overset{notation}{=} C_{stab}\,. \end{aligned} \tag{4.3}$$

Proof. Setting $\varphi = u_R^{j,n+1}$ and using the skew-symmetry of the trilinear term we have

$$\begin{aligned} &\frac{1}{2}\|u_R^{j,n+1}\|^2 - \frac{1}{2}\|u_R^{j,n}\|^2 + \frac{1}{2}\|u_R^{j,n+1} - u_R^{j,n}\|^2 + \nu_{max}\Delta t\|\nabla u_R^{j,n+1}\|^2 \\ &\quad + \Delta t b^*(\overline{u_R^{j,n} - < u_R >^n}, u_R^{j,n}, u_R^{j,n+1} - u_R^{j,n}) \\ &\quad = \Delta t(f_j^{n+1}, u_R^{j,n+1}) - \Delta t(\nu_j - \nu_{max})\left(\nabla u_R^{j,n}, \nabla u_R^{j,n+1}\right). \end{aligned} \tag{4.4}$$

Now applying Young's inequality on the right-hand side we have

$$\begin{aligned} &\frac{1}{2}\|u_R^{j,n+1}\|^2 - \frac{1}{2}\|u_R^{j,n}\|^2 + \frac{1}{2}\|u_R^{j,n+1} - u_R^{j,n}\|^2 + \nu_{max}\Delta t\|\nabla u_R^{j,n+1}\|^2 \\ &+ \Delta t b^*(\overline{u_R^{j,n} - < u_R >^n}, u_R^{j,n}, u_R^{j,n+1} - u_R^{j,n}) \leqslant \frac{\alpha\,\Delta t \nu_{max}}{4}\|\nabla u_R^{j,n+1}\|^2 \\ &+ \frac{\Delta t}{\alpha\,\nu_{max}}\|f_j^{n+1}\|_{-1}^2 + \frac{\beta\,\Delta t\nu_{max}}{4}\|\nabla u_R^{j,n+1}\|^2 + \frac{\Delta t(\nu_j - \nu_{max})^2}{\beta\,\nu_{max}}\|\nabla u_R^{j,n}\|^2. \end{aligned} \tag{4.5}$$

Since both $\frac{\beta\,\Delta t\nu_{max}}{4}\|\nabla u_R^{j,n+1}\|^2$ and $\frac{\Delta t(\nu_j - \nu_{max})^2}{\beta\nu_{max}}\|\nabla u_R^{j,n}\|^2$ need to be absorbed into $\nu_{max}\Delta t\|u_R^{j,n+1}\|^2$, we minimize the quantity $\frac{\beta\,\Delta t\nu_{max}}{4} + \frac{\Delta t(\nu_j - \nu_{max})^2}{\beta\nu_{max}}$ by selecting $\beta = \frac{2|\nu_j - \nu_{max}|}{\nu_{max}}$. It then follows that

$$\begin{aligned} &\frac{1}{2}\|u_R^{j,n+1}\|^2 - \frac{1}{2}\|u_R^{j,n}\|^2 + \frac{1}{2}\|u_R^{j,n+1} - u_R^{j,n}\|^2 + \nu_{max}\Delta t\|\nabla u_R^{j,n+1}\|^2 \\ &+ \Delta t b^*(\overline{u_R^{j,n} - < u_R >^n}, u_R^{j,n}, u_R^{j,n+1} - u_R^{j,n}) \leqslant \frac{\alpha\,\Delta t \nu_{max}}{4}\|\nabla u_R^{j,n+1}\|^2 \\ &+ \frac{\Delta t}{\alpha\,\nu_{max}}\|f_j^{n+1}\|_{-1}^2 + \frac{\Delta t|\nu_j - \nu_{max}|}{2}\|\nabla u_R^{j,n+1}\|^2 + \frac{\Delta t|\nu_j - \nu_{max}|}{2}\|\nabla u_R^{j,n}\|^2. \end{aligned} \tag{4.6}$$

Next we bound the trilinear term using (2.3) and (3.3), obtaining

$$
\begin{aligned}
&-\Delta t b^*(\overline{u_R^{j,n} - < u_R >^n}, u_R^{j,n}, u_R^{j,n+1} - u_R^{j,n}) \\
&\quad \leqslant C_{b^*}\Delta t \|\overline{u_R^{j,n} - < u_R >^n}\| \|\nabla u_R^{j,n}\| \left(\|\nabla(u_R^{j,n+1} - u_R^{j,n})\| \|u_R^{j,n+1} - u_R^{j,n}\|\right)^{\frac{1}{2}} \\
&\quad \leqslant C_{b^*}\Delta t |||\mathbb{S}_R|||_2^{\frac{1}{4}} \|\overline{u_R^{j,n} - < u_R >^n}\| \|\nabla u_R^{j,n}\| \|u_R^{j,n+1} - u_R^{j,n}\|. \qquad (4.7)
\end{aligned}
$$

Then using Young's inequality we obtain

$$
\begin{aligned}
&-\Delta t b^*(\overline{u_R^{j,n} - < u_R >^n}, u_R^{j,n}, u_R^{j,n+1} - u_R^{j,n}) \\
&\quad \leqslant \frac{C_{b^*}^2 \Delta t^2}{2} |||\mathbb{S}_R|||_2^{\frac{1}{2}} \|\overline{u_R^{j,n} - < u_R >^n}\|^2 \|\nabla u_R^{j,n}\|^2 + \frac{1}{2}\|u_R^{j,n+1} - u_R^{j,n}\|^2. \qquad (4.8)
\end{aligned}
$$

Combining like terms we then have

$$
\begin{aligned}
&\frac{1}{2}\|u_R^{j,n+1}\|^2 - \frac{1}{2}\|u_R^{j,n}\|^2 + \nu_{max}\Delta t\left(1 - \frac{\alpha}{4} - \frac{|\nu_j - \nu_{max}|}{2\nu_{max}}\right)\|\nabla u_R^{j,n+1}\|^2 \\
&\leqslant \frac{\Delta t}{\alpha\nu_{max}}\|f_j^{n+1}\|_{-1}^2 + \frac{C_{b^*}^2 \Delta t^2}{2} |||\mathbb{S}_R|||_2^{\frac{1}{2}} \|\overline{u_R^{j,n} - < u_R >^n}\|^2 \|\nabla u_R^{j,n}\|^2 \\
&\quad + \frac{\Delta t|\nu_j - \nu_{max}|}{2}\|\nabla u_R^{j,n}\|^2. \qquad (4.9)
\end{aligned}
$$

Rearranging terms it follows that

$$
\begin{aligned}
&\frac{1}{2}\|u_R^{j,n+1}\|^2 - \frac{1}{2}\|u_R^{j,n}\|^2 + \nu_{max}\Delta t\Bigg(\left(1 - \frac{\alpha}{4} - \frac{|\nu_j - \nu_{max}|}{2\nu_{max}}\right)\|\nabla u_R^{j,n+1}\|^2 \\
&-\left(\frac{|\nu_j - \nu_{max}|}{2\nu_{max}} + \frac{C_{b^*}^2 \Delta t}{2\,\nu_{max}} |||\mathbb{S}_R|||_2^{\frac{1}{2}} \|\overline{u_R^{j,n} - < u_R >^n}\|^2\right)\|\nabla u_R^{j,n}\|^2\Bigg) \leqslant \frac{\Delta t}{\alpha\nu_{max}}\|f_j^{n+1}\|_{-1}^2. \qquad (4.10)
\end{aligned}
$$

Using the fact that $\max\limits_{1\leqslant j\leqslant J} \frac{|\nu_j - \nu_{max}|}{\nu_{max}} = 1 - \epsilon$ for $0 \leqslant \varepsilon \leqslant 1$ and taking $\alpha = \epsilon$ we have

$$
\begin{aligned}
&\frac{1}{2}\|u_R^{j,n+1}\|^2 - \frac{1}{2}\|u_R^{j,n}\|^2 + \nu_{max}\Delta t\Bigg(\left(\frac{1}{2} + \frac{\varepsilon}{4}\right)\|\nabla u_R^{j,n+1}\|^2 \\
&-\left(\frac{1}{2} - \frac{\varepsilon}{2} + \frac{C_{b^*}^2 \Delta t}{2\,\nu_{max}} |||\mathbb{S}_R|||_2^{\frac{1}{2}} \|\overline{u_R^{j,n} - < u_R >^n}\|^2\right)\|\nabla u_R^{j,n}\|^2\Bigg) \leqslant \frac{\Delta t}{\nu_{max}\varepsilon}\|f_j^{n+1}\|_{-1}^2. \qquad (4.11)
\end{aligned}
$$

Now using assumption (4.2), (4.11) we have

$$
\begin{aligned}
&\frac{1}{2}\|u_R^{j,n+1}\|^2 - \frac{1}{2}\|u_R^{j,n}\|^2 + \nu_{max}\Delta t\left(\frac{1}{2}\|\nabla u_R^{j,n+1}\|^2 - \frac{1}{2}\|\nabla u_R^{j,n}\|^2\right) \\
&\quad + \nu_{max}\Delta t\frac{\varepsilon}{4}\|u_R^{j,n+1}\|^2 \leqslant \frac{\Delta t}{\nu_{max}\varepsilon}\|f_j^{n+1}\|_{-1}^2. \qquad (4.12)
\end{aligned}
$$

Summing up (4.12) from 0 to $N-1$ yields (4.3). □

REMARK 4.2 The term ε in the above theorem measures the relative uncertainty present in the viscosities. In practice the amount of uncertainty present in the viscosities can be one or two orders of magnitude. In this case $\varepsilon \approx \mathcal{O}(10^{-1})$ or $\mathcal{O}(10^{-2})$.

REMARK 4.3 The reason we see an improvement in the stability from the use of ν_{max} is that the quantity $\max\limits_{1\leqslant j\leqslant J} \frac{|\nu_j-\nu_{max}|}{\nu_{max}} \leqslant 1$. When the average $< \nu >$ is used instead, the corresponding quantity $\max\limits_{1\leqslant j\leqslant J} \frac{|\nu_j-<\nu>|}{<\nu>}$ can be much greater than 1.

REMARK 4.4 The stability improvement from ν_{max} will also apply in the case of full finite element solutions. The proof for this will be identical to the proof for Theorem 4.1.

5. Error analysis

We next provide an error analysis for Leray ensemble-POD solutions. First, we present several results obtained in Gunzburger *et al.* (2017), which we use in the analysis. We also use the following notation.

DEFINITION 5.1 (Generic Constant C). Let C be a generic constant that can depend on f, u^j, but not on $h, \Delta t, R, \lambda_i, \varepsilon, \nu_{max}, \delta, C_{stab}, C_{b^*}$.

The following lemma is similar to Gunzburger *et al.* (2017, Lemma 5.1).

LEMMA 5.2 [$L^2(\Omega)$ norm of the error between snapshots and their projections onto the POD space.] We have

$$\frac{1}{J_S(N_S+1)} \sum_{j=1}^{J_S} \sum_{m=0}^{N_S} \left\| u_{h,S}^{j,m} - \sum_{i=1}^{R} (u_{h,S}^{j,m}, \varphi_i)\varphi_i \right\|^2 = \sum_{i=R+1}^{J_S(N_S+1)} \lambda_i$$

and thus for $j = 1, \ldots, J_S$

$$\frac{1}{N_S+1} \sum_{m=0}^{N_S} \left\| u_{h,S}^{j,m} - \sum_{i=1}^{R} (u_{h,S}^{j,m}, \varphi_i)\varphi_i \right\|^2 \leqslant J_S \sum_{i=R+1}^{J_S(N_S+1)} \lambda_i.$$

The following lemma is similar to Gunzburger *et al.* (2017, Lemma 5.2).

LEMMA 5.3 [$H^1(\Omega)$ norm of the error between snapshots and their projections in the POD space.] We have

$$\frac{1}{J_S(N_S+1)} \sum_{j=1}^{J_S} \sum_{m=0}^{N_S} \left\| \nabla \left(u_{h,S}^{j,m} - \sum_{i=1}^{R} (u_{h,S}^{j,m}, \varphi_i)\varphi_i \right) \right\|^2 = \sum_{i=R+1}^{J_S(N_S+1)} \lambda_i \|\nabla \varphi_i\|^2$$

and thus, for $j = 1, \ldots, J_S$,

$$\frac{1}{N_S+1} \sum_{m=0}^{N_S} \left\| \nabla \left(u_{h,S}^{j,m} - \sum_{i=1}^{R} (u_{h,S}^{j,m}, \varphi_i)\varphi_i \right) \right\|^2 \leqslant J_S \sum_{i=R+1}^{J_S(N_S+1)} \lambda_i \|\nabla \varphi_i\|^2.$$

The following lemma is similar to Gunzburger *et al.* (2017, Lemma 5.3) (see also Iliescu & Wang (2014, Lemma 3.3)).

LEMMA 5.4 [Error in the projection onto the POD space.] Consider the partition $0 = t_0 < t_1 < \cdots < t_{N_S} = T$ used in Section 3. For any $u \in H^1(0,T;[H^{s+1}(\Omega)]^d)$ let $u^m = u(\cdot, t_m)$. Then, the error in the projection onto the POD space X_R satisfies the estimates

$$\frac{1}{N_S+1}\sum_{m=0}^{N_S}\|u^{j,m}-P_Ru^{j,m}\|^2 \leqslant C\left(h^{2s+2}+\Delta t^4\right)+J_S\sum_{i=R+1}^{J_S(N_S+1)}\lambda_i$$

$$\frac{1}{N_S+1}\sum_{m=0}^{N_S}\left\|\nabla\left(u^{j,m}-P_Ru^{j,m}\right)\right\|^2 \leqslant (C+h^2|||\mathbb{S}_R|||_2)h^{2s}+(C+|||\mathbb{S}_R|||_2)\Delta t^4+J_S\sum_{i=R+1}^{J_S(N_S+1)}\|\nabla\varphi_i\|^2\lambda_i.$$

We assume the following estimates are also valid, as done in Iliescu & Wang (2014).

ASSUMPTION 5.5 Consider the partition $0 = t_0 < t_1 < \cdots < t_{N_S} = T$ used in Section 3. For any $u \in H^1(0,T;[H^{s+1}(\Omega)]^d)$ let $u^m = u(\cdot, t_m)$. Then, the error in the projection onto the POD space X_R satisfies the estimates

$$\|u^{j,m}-P_Ru^{j,m}\|^2 \leqslant C\left(h^{2s+2}+\Delta t^4\right)+J_S\sum_{i=R+1}^{J_S(N_S+1)}\lambda_i$$

$$\left\|\nabla\left(u^{j,m}-P_Ru^{j,m}\right)\right\|^2 \leqslant (C+h^2|||\mathbb{S}_R|||_2)h^{2s}+(C+|||\mathbb{S}_R|||_2)\Delta t^4+J_S\sum_{i=R+1}^{J_S(N_S+1)}\|\nabla\varphi_i\|^2\lambda_i.$$

Next we need to make an assumption on the regularity of $u_R^{j,m}$ in order to establish an estimate for the ROM filtering error. We note that this assumption is consistent with our regularity Assumption 2.1.

ASSUMPTION 5.6 We assume that $\Delta u_R^{j,m} \in L^2$.

We now state an estimate for the ROM filtering error that is a simple extension of Xie *et al.* (2018, Lemma 4.3).

LEMMA 5.7 [ROM filtering error estimates.] If $\Delta u_R^{j,m} \in L^2$ then the following estimate holds:

$$\begin{aligned}&\delta^2\|\nabla(u_R^{j,m}-\overline{u_R^{j,m}})\|^2+\|u_R^{j,m}-\overline{u_R^{j,m}}\|^2\\ &\leqslant C\left(C\left(h^{2s+2}+\Delta t^4\right)+J_S\sum_{i=R+1}^{J_S(N_S+1)}\lambda_i\right)\\ &\quad+C\delta^2\left((C+h^2|||\mathbb{S}_R|||_2)h^{2s}+(C+|||\mathbb{S}_R|||_2)\Delta t^4+J_S\sum_{i=R+1}^{J_S(N_S+1)}\|\nabla\varphi_i\|^2\lambda_i\right)\\ &\quad+C\delta^4\|\Delta u_R^{j,m}\|^2. \end{aligned} \tag{5.1}$$

Lastly, we state a result for the stability of the ROM filtered variables proven in Xie *et al.* (2018, Lemma 4.4).

LEMMA 5.8 [ROM stability estimates.] For $u \in X$ we have

$$\begin{aligned} \|\overline{u}\| &\leqslant \|u\| \\ \|\nabla \overline{u}\| &\leqslant |||S_R|||_2^{\frac{1}{2}} \|u\|. \end{aligned} \tag{5.2}$$

For $u \in X_R$ we have

$$\|\nabla \overline{u}\| \leqslant \|\nabla u\|. \tag{5.3}$$

Let $e^{j,n} = u^{j,n} - u_R^{j,n}$ denote the error between the true solution and the POD approximation; then, we have the following error estimates.

THEOREM 5.9 Consider the Leray ensemble-POD algorithm (3.6) and the partition $0 = t_0 < t_1 < \cdots < t_{N_S}$ used in Section 3. Suppose for any $0 \leqslant n \leqslant N_S$ the stability conditions from Theorem 4.1 and all previously stated regularity assumptions hold. Then for any $1 \leqslant N \leqslant N_S$ there is a positive constant C, such that the following bound holds:

$$\begin{aligned} &\frac{1}{2}\|e^{j,N}\|^2 + \frac{\nu_{max}}{2}\|\nabla e^{j,N}\|^2 + \frac{\varepsilon}{4}\nu_{max}\|\nabla e^{j,N}\|^2 + C\nu_{max}\Delta t\sum_{n=0}^{N-1}\|e^{j,n+1}\|^2 \\ &\leqslant \exp\left(\frac{C_{b^*}^4\, C^4\, T}{\varepsilon^3\, \nu_{max}^3}\right)\Bigg[\left(\frac{C\,\nu_{max}\Delta t}{\varepsilon} + \frac{C\Delta t}{\varepsilon}\frac{|\nu_j - \nu_{max}|^2}{\nu_{max}} + 2C|||\mathbb{S}_R|||_2^{-\frac{1}{2}} + \frac{C\,C_{b^*}^2\,\Delta t}{\varepsilon\,\nu_{max}}\right. \\ &\quad \left. + \frac{C\,C_{b^*}^2\,C_{stab}}{2\,\varepsilon\,\nu_{max}} + \frac{2\,C\,C_{b^*}^2\,C_{stab}^2}{\varepsilon^2\,\nu_{max}^2} + \frac{C\,C_{b^*}^2\,\delta}{\varepsilon\,\nu_{max}}\right) \\ &\quad \times \left((C + h^2|||\mathbb{S}_R|||_2)h^{2s} + (C + |||\mathbb{S}_R|||_2)\Delta t^4 + J_S\sum_{i=R+1}^{J_S(N_S+1)}\|\nabla\varphi_i\|^2\lambda_i\right) \\ &\quad + \frac{C\,C_{b^*}^2}{\delta\,\varepsilon\,\nu_{max}}\left(C\left(h^{2s+2} + \Delta t^4\right) + J_S\sum_{i=R+1}^{J_S(N_S+1)}\lambda_i\right) \\ &\quad + \frac{C\,\Delta t^2}{\varepsilon}\frac{|\nu_j - \nu_{max}|^2}{\nu_{max}} + C\Delta t|||\mathbb{S}_R|||_2^{-\frac{1}{2}} + \frac{Ch^{2s}}{d\,\varepsilon\,\nu_{max}}\|\|p^j\|\|_{2,s}^2 + \frac{C\Delta t^2}{\varepsilon\,\nu_{max}} \\ &\quad + \frac{C\,C_{b^*}^2\,\Delta t^2}{\varepsilon\,\nu_{max}} + \frac{C\,C_{b^*}^2\,\Delta t\,\delta^3}{\varepsilon\,\nu_{max}}\Bigg] \\ &\quad + \left(1 + CN\nu_{max}\Delta t\right) \times \left(C\left(h^{2s+2} + \Delta t^4\right) + J_S\sum_{i=R+1}^{J_S(N_S+1)}\lambda_i\right) \\ &\quad + \left(\nu_{max} + \frac{\varepsilon}{2}\nu_{max}\right) \times \left((C + h^2|||\mathbb{S}_R|||_2)h^{2s} + (C + |||\mathbb{S}_R|||_2)\Delta t^4 + J_S\sum_{i=R+1}^{J_S(N_S+1)}\|\nabla\varphi_i\|^2\lambda_i\right). \end{aligned} \tag{5.4}$$

Proof. The weak solution of the NSE u^j satisfies

$$\left(\frac{u^{j,n+1}-u^{j,n}}{\Delta t},\varphi\right)+b^*(u^{j,n+1},u^{j,n+1},\varphi)+\nu_j(\nabla u^{j,n+1},\nabla\varphi)-(p^{j,n+1},\nabla\cdot\varphi)$$
$$=(f^{j,n+1},\varphi)+Int\,p(u^{j,n+1};\varphi), \tag{5.5}$$

where

$$Int\,p(u^{j,n+1};\varphi)=\left(\frac{u^{j,n+1}-u^{j,n}}{\Delta t}-u_t^j(t^{n+1}),\varphi\right). \tag{5.6}$$

We split the error

$$e^{j,n}=u^{j,n}-u_R^{j,n}=(u^{j,n}-P_Ru^{j,n})+(P_Ru^{j,n}-u_R^{j,n})=\eta^{j,n}+\xi_R^{j,n},\qquad j=1,\ldots,J. \tag{5.7}$$

Subtracting (3.6) from (5.5) as well as adding and subtracting the terms $\nu_{max}(\nabla u_j^{n+1},\nabla\varphi)$ and $\nu_j-\nu_{max}(\nabla u_j^{n+1},\nabla\varphi)$ we have

$$\left(\frac{\xi_R^{j,n+1}-\xi_R^{j,n}}{\Delta t},\varphi\right)+\nu_{max}(\nabla\xi_R^{j,n+1},\nabla\varphi)+(\nu_j-\nu_{max})(\nabla(u^{j,n+1}-u^{j,n}),\nabla\varphi)$$
$$+(\nu_j-\nu_{max})(\nabla\xi_R^{j,n},\nabla\varphi)+b^*(u^{j,n+1},u^{j,n+1},\varphi)-b^*(\overline{<u_R>^n},u_R^{j,n+1},\varphi)$$
$$-b^*(\overline{u_R^{j,n}-<u_R>^n},u_R^{j,n},\varphi)-(p^{j,n+1},\nabla\cdot\varphi)$$
$$=-\left(\frac{\eta^{j,n+1}-\eta^{j,n}}{\Delta t},\varphi\right)-\nu_{max}(\nabla\eta^{j,n+1},\nabla\varphi)-(\nu_j-\nu_{max})(\nabla\eta^{j,n},\nabla\varphi)+Intp(u^{j,n+1};\varphi). \tag{5.8}$$

Setting $\varphi=\xi_R^{j,n+1}$, rearranging the nonlinear terms by adding and subtracting $b^*\left(\overline{u_R^{j,n}-<u_R>^n},u_R^{j,n+1},\xi_R^{j,n+1}\right)$ and using the fact that $(\eta^{j,n+1}-\eta^{j,n},\xi_R^{j,n+1})=0$ by the definition of the L^2 projection we have

$$\frac{1}{\Delta t}\left(\frac{1}{2}\|\xi_R^{j,n+1}\|^2-\frac{1}{2}\|\xi_R^{j,n}\|^2+\frac{1}{2}\|\xi_R^{j,n+1}-\xi_R^{j,n}\|^2\right)+\nu_{max}\|\nabla\xi_R^{j,n+1}\|^2$$
$$=-(\nu_j-\nu_{max})(\nabla(u^{j,n+1}-u^{j,n}),\nabla\xi_R^{j,n+1})-(\nu_j-\nu_{max})(\nabla\xi_R^{j,n},\nabla\xi_R^{j,n+1})$$
$$-\nu_{max}(\nabla\eta^{j,n+1},\nabla\xi_R^{j,n+1})-(\nu_j-\nu_{max})(\nabla\eta^{j,n},\nabla\xi_R^{j,n+1})$$
$$+b^*(\overline{u_R^{j,n}},u_R^{j,n+1},\xi_R^{j,n+1})-b^*(\overline{u_R^{j,n}-<u_R>^n},u_R^{j,n+1}-u_R^{j,n},\xi_R^{j,n+1})$$
$$-b^*(u^{j,n+1},u^{j,n+1},\xi_R^{j,n+1})+(p^{j,n+1},\nabla\cdot\xi_R^{j,n+1})+Intp(u^{j,n+1};\xi_R^{j,n+1}). \tag{5.9}$$

We bound the viscous terms in a similar manner to Gunzburger *et al.* (2017b, Theorem 3.1)

$$-(\nu_j-\nu_{max})(\nabla(u^{j,n+1}-u^{j,n}),\nabla\xi_R^{j,n+1}) \leqslant \frac{\Delta t}{4\tilde{\epsilon}}\frac{|\nu_j-\nu_{max}|^2}{\nu_{max}}\left(\int_{t^n}^{t^n+1}\|\nabla u_{j,t}\|^2\,\mathrm{d}t\right)+\tilde{\epsilon}\nu_{max}\|\nabla\xi_R^{j,n+1}\|^2, \tag{5.10}$$

$$-\nu_{max}(\nabla\eta^{j,n+1},\nabla\xi_R^{j,n+1}) \leqslant \frac{\nu_{max}}{4\tilde{\epsilon}}\|\nabla\eta^{j,n+1}\|^2+\tilde{\epsilon}\nu_{max}\|\nabla\xi_R^{j,n+1}\|^2, \tag{5.11}$$

$$-(\nu_j-\nu_{max})(\nabla\eta^{j,n},\nabla\xi_R^{j,n+1}) \leqslant \frac{1}{4\tilde{\epsilon}}\frac{|\nu_j-\nu_{max}|^2}{\nu_{max}}\|\nabla\eta^{j,n}\|^2+\tilde{\epsilon}\nu_{max}\|\nabla\xi_R^{j,n+1}\|^2, \tag{5.12}$$

$$-(\nu_j-\nu_{max})(\nabla\xi_R^{j,n},\nabla\xi_R^{j,n+1}) \leqslant \frac{|\nu_j-\nu_{max}|}{2}\|\nabla\xi_R^{j,n}\|^2+\frac{|\nu_j-\nu_{max}|}{2}\|\nabla\xi_R^{j,n+1}\|^2. \tag{5.13}$$

We next rewrite the second nonlinear term on the right-hand side of (5.9).

$$\begin{aligned}
&b^*(\overline{u_R^{j,n}-<u_R>^n},u_R^{j,n+1}-u_R^{j,n},\xi_R^{j,n+1})\\
&\quad=-b^*(\overline{u_R^{j,n}-<u_R>^n},e^{j,n+1}-e^{j,n},\xi_R^{j,n+1})\\
&\qquad+b^*(\overline{u_R^{j,n}-<u_R>^n},u^{j,n+1}-u^{j,n},\xi_R^{j,n+1})\\
&\quad=-b^*(\overline{u_R^{j,n}-<u_R>^n},\eta^{j,n+1},\xi_R^{j,n+1})\\
&\qquad+b^*(\overline{u_R^{j,n}-<u_R>^n},\eta^{j,n},\xi_R^{j,n+1})\\
&\qquad+b^*(\overline{u_R^{j,n}-<u_R>^n},\xi_R^{j,n},\xi_R^{j,n+1})\\
&\qquad+b^*(\overline{u_R^{j,n}-<u_R>^n},u^{j,n+1}-u^{j,n},\xi_R^{j,n+1}).
\end{aligned} \tag{5.14}$$

As done in Gunzburger *et al.* (2017b, Theorem 3.1), using Young's inequality (2.3), (2.4) and (3.3) we derive the estimates

$$\begin{aligned}
&-b^*(\overline{u_R^{j,n}-<u_R>^n},\eta^{j,n+1},\xi_R^{j,n+1})\\
&\quad\leqslant\frac{C_{b^*}^2\nu_{max}^{-1}}{4\tilde{\epsilon}}\|\nabla(\overline{u_R^{j,n}-<u_R>^n})\|^2\|\nabla\eta^{j,n+1}\|^2+\tilde{\epsilon}\nu_{max}\|\nabla\xi_R^{j,n+1}\|^2,
\end{aligned} \tag{5.15}$$

$$b^*(\overline{u_R^{j,n} - < u_R >^n}, \eta^{j,n}, \xi_R^{j,n+1}) \leqslant \frac{C_{b^*}^2 \nu_{max}^{-1}}{4\tilde{\epsilon}} \|\nabla(\overline{u_R^{j,n} - < u_R >^n})\|^2 \|\nabla \eta^{j,n}\|^2 + \tilde{\epsilon} \nu_{max} \|\nabla \xi_R^{j,n+1}\|^2, \tag{5.16}$$

$$b^*(\overline{u_R^{j,n} - < u_R >^n}, u^{j,n+1} - u^{j,n}, \xi_R^{j,n+1}) \leqslant \frac{C\, C_{b^*}^2 \nu_{max}^{-1}}{4\tilde{\epsilon}} \Delta t \|\nabla(\overline{u_R^{j,n} - < u_R >^n})\|^2 + \tilde{\epsilon} \nu_{max} \|\nabla \xi_R^{j,n+1}\|^2. \tag{5.17}$$

By skew-symmetry, inequality (2.4) and the inverse inequality (3.3) we have

$$\begin{aligned} b^*(\overline{u_R^{j,n} - < u_R >^n}, \xi_R^{j,n}, \xi_R^{j,n+1}) &\leqslant C_{b^*} \|\nabla(\overline{u_R^{j,n} - < u_R >^n})\| \|\nabla \xi_R^{j,n}\| \sqrt{\|\xi_R^{j,n+1} - \xi_R^{j,n}\| \|\nabla(\xi_R^{j,n+1} - \xi_R^{j,n})\|} \\ &\leqslant C_{b^*} \|\|\mathbb{S}_R\|\|_2^{1/4} \|\nabla(\overline{u_R^{j,n} - < u_R >^n})\| \|\nabla \xi_R^{j,n}\| \|\xi_R^{j,n+1} - \xi_R^{j,n}\| \\ &\leqslant \frac{1}{2\Delta t} \|\xi_R^{j,n+1} - \xi_R^{j,n}\|^2 + \left(\frac{C_{b^*}^2 \Delta t}{2} \|\|\mathbb{S}_R\|\|_2^{\frac{1}{2}} \|\nabla(\overline{u_R^{j,n} - < u_R >^n})\|^2 \right) \|\nabla \xi_R^{j,n}\|^2. \end{aligned} \tag{5.18}$$

Bounding the other two nonlinear terms, we add and subtract the terms $b^*(u^{j,n}, u^{j,n+1}, \xi_R^{j,n+1})$ and $b^*(\overline{u_R^{j,n}}, u^{j,n+1}, \xi_R^{j,n+1})$. It then follows from (2.3)

$$\begin{aligned} &- b^*(u^{j,n+1}, u^{j,n+1}, \xi_R^{j,n+1}) + b^*(\overline{u_R^{j,n}}, u_R^{j,n+1}, \xi_R^{j,n+1}) \\ &= -b^*(u^{j,n} - \overline{u_R^{j,n}}, u^{j,n+1}, \xi_R^{j,n+1}) - b^*(\overline{u_R^{j,n}}, \eta^{j,n+1}, \xi_R^{j,n+1}) \\ &- b^*(u^{j,n+1} - u^{j,n}, u^{j,n+1}, \xi_R^{j,n+1}). \end{aligned} \tag{5.19}$$

Now by Young's inequality, (2.4), the stability analysis, i.e., $\|\overline{u_R^{j,n}}\|^2 \leqslant C_{stab}$, and the assumption $u^j \in L^\infty(0, T, H^1(\Omega))$ we have

$$\begin{aligned} b^*(\overline{u_R^{j,n}}, \eta^{j,n+1}, \xi_R^{j,n+1}) &\leqslant C_{b^*} \|\nabla \overline{u_R^{j,n}}\|^{\frac{1}{2}} \|\overline{u_R^{j,n}}\|^{\frac{1}{2}} \|\nabla \eta^{j,n+1}\| \|\nabla \xi_R^{j,n+1}\| \\ &\leqslant \frac{C_{stab} C_{b^*}^2}{4\tilde{\epsilon}} \nu_{max}^{-1} \|\nabla \overline{u_R^{j,n}}\| \|\nabla \eta^{j,n+1}\|^2 + \tilde{\epsilon} \nu_{max} \|\nabla \xi_R^{j,n+1}\|^2, \end{aligned} \tag{5.20}$$

as well as

$$b^*(u^{j,n+1} - u^{j,n}, u^{j,n+1}, \xi_R^{j,n+1}) \leqslant \frac{C\, C_{b^*}^2 \Delta t}{4\tilde{\epsilon}} \nu_{max}^{-1} + \tilde{\epsilon} \nu_{max} \|\nabla \xi_R^{j,n+1}\|^2. \tag{5.21}$$

We can then rewrite the term

$$- b^*(u^{j,n} - \overline{u_R^{j,n}}, u^{j,n+1}, \xi_R^{j,n+1}) = - b^*(e^{j,n}, u^{j,n+1}, \xi_R^{j,n+1}) - b^*(u_R^{j,n} - \overline{u_R^{j,n}}, u^{j,n+1}, \xi_R^{j,n+1}). \quad (5.22)$$

Bounding the second term

$$\begin{aligned} &- b^*(u_R^{j,n} - \overline{u_R^{j,n}}, u^{j,n+1}, \xi_R^{j,n+1}) \\ &\quad \leqslant C_{b^*} \|u_R^{j,n} - \overline{u_R^{j,n}}\|^{\frac{1}{2}} \|\nabla(u_R^{j,n} - \overline{u_R^{j,n}})\|^{\frac{1}{2}} \|\nabla u^{j,n+1}\| \|\nabla \xi_R^{j,n+1}\| \\ &\quad \leqslant \frac{C_{b^*}^2}{4\tilde{\epsilon}} \nu_{max}^{-1} \|u_R^{j,n} - \overline{u_R^{j,n}}\| \|\nabla(u_R^{j,n} - \overline{u_R^{j,n}})\| \|\nabla u^{j,n+1}\|^2 + \tilde{\epsilon} \nu_{max} \|\nabla \xi_R^{j,n+1}\|^2. \end{aligned} \quad (5.23)$$

Then after decomposing $e^{j,n} = \eta^{j,n} + \xi_R^{j,n}$ again using Young's inequality and the assumption $u^j \in L^\infty(0, T, H^1(\Omega))$

$$- b^*(\eta^{j,n}, u^{j,n+1}, \xi_R^{j,n+1}) \leqslant \frac{C C_{b^*}^2}{4\tilde{\epsilon}} \nu_{max}^{-1} \|\nabla \eta^{j,n}\|^2 + \tilde{\epsilon} \nu_{max} \|\nabla \xi_R^{j,n+1}\|^2 \quad (5.24)$$

and

$$\begin{aligned} -b^*(\xi_R^{j,n}, u^{j,n+1}, \xi_R^{j,n+1}) &\leqslant C_{b^*} \|\nabla \xi_R^{j,n}\|^{\frac{1}{2}} \|\xi_R^{j,n}\|^{\frac{1}{2}} \|\nabla u^{j,n+1}\| \|\nabla \xi_R^{j,n+1}\| \\ &\leqslant C_{b^*} C \left(\alpha \|\nabla \xi_R^{j,n+1}\|^2 + \frac{1}{4\alpha} \|\nabla \xi_R^{j,n}\| \|\xi_R^{j,n}\| \right). \\ &\leqslant C_{b^*} C \left(\alpha \|\nabla \xi_R^{j,n+1}\|^2 + \frac{1}{4\alpha} \left(\beta \|\nabla \xi_R^{j,n}\|^2 + \frac{1}{\beta} \|\xi_R^{j,n}\|^2 \right) \right) \\ &= \tilde{\epsilon} \nu_{max} \|\nabla \xi_R^{j,n+1}\|^2 + \frac{13\,\tilde{\epsilon}}{4} \nu_{max} \|\nabla \xi_R^{j,n}\|^2 + \frac{C_{b^*}^4 C^4}{52\, \nu_{max}^3 \tilde{\epsilon}^3} \|\xi_R^{j,n}\|^2. \end{aligned} \quad (5.25)$$

For the pressure term since $\xi_{j,r}^{n+1} \in X^R \subset V^h$ it follows for $q_h \in Q^h$

$$\begin{aligned} (p_j^{n+1}, \nabla \cdot \xi_R^{j,n+1}) =& (p^{j,n+1} - q_h^{n+1}, \nabla \cdot \xi_R^{j,n+1}) \\ &\leqslant \tilde{\epsilon} \nu_{max} \|\nabla \xi_R^{n+1}\|^2 + \frac{\nu_{max}^{-1}}{4d\tilde{\epsilon}} \|p^{j,n+1} - q_h^{j,n+1}\|^2. \end{aligned} \quad (5.26)$$

For the last term we have

$$\begin{aligned} Intp(u^{j,n+1}, \xi_R^{j,n+1}) &\leqslant \left\| \frac{u^{j,n+1} - u^{j,n}}{\Delta t} - u_t^j(t^{n+1}) \right\| \|\nabla \xi_R^{j,n+1}\| \\ &\leqslant \frac{C\Delta t}{4\tilde{\epsilon}} \nu_{max}^{-1} t + \tilde{\epsilon} \nu_{max} \|\nabla \xi_R^{j,n+1}\|^2. \end{aligned} \quad (5.27)$$

Now combining (5.10)–(5.27) (5.9) becomes

$$
\begin{aligned}
&\frac{1}{\Delta t}\left(\frac{1}{2}\|\xi_R^{j,n+1}\|^2-\frac{1}{2}\|\xi_R^{j,n}\|^2\right)\\
&\quad+\nu_{max}\|\nabla\xi_R^{j,n+1}\|^2-\frac{C_{b^*}^2\Delta t}{2}\|\|\mathbb{S}_R\|\|_2^{\frac{1}{2}}\|\nabla(\overline{u_R^{j,n}-<u_R>^n})\|^2\,\|\nabla\xi_R^{j,n}\|^2\\
&\quad-\frac{13\tilde{\epsilon}}{4}\nu_{max}\|\nabla\xi_R^{j,n+1}\|^2-\frac{13\tilde{\epsilon}}{4}\,\nu_{max}\|\nabla\xi_R^{j,n}\|^2\\
&\quad-\frac{|\nu_j-\nu_{max}|}{2}\|\nabla\xi_R^{j,n+1}\|^2-\frac{|\nu_j-\nu_{max}|}{2}\|\nabla\xi_R^{j,n}\|^2\\
&\leqslant\frac{C_{b^*}^4\,C^4}{52\,\nu_{max}^3\,\tilde{\epsilon}^3}\|\xi_R^{j,n}\|^2+\frac{C\Delta t}{4\,\tilde{\epsilon}}\frac{|\nu_j-\nu_{max}|^2}{\nu_{max}}+\frac{\nu_{max}}{4\,\tilde{\epsilon}}\,\|\nabla\eta^{j,n+1}\|^2\\
&\quad+\frac{CC_{b^*}^2\,\Delta t}{4\,\tilde{\epsilon}\,\nu_{max}}\|\nabla(\overline{u_R^{j,n}-<u_R>^n})\|^2\\
&\quad+\frac{1}{4\,d\,\tilde{\epsilon}\,\nu_{max}}\|p^{j,n+1}-q_h^{n+1}\|^2+\frac{C\Delta t}{4\,\tilde{\epsilon}\,\nu_{max}}\\
&\quad+\frac{CC_{b^*}^2\,\Delta t}{4\,\tilde{\epsilon}\nu_{max}}+\frac{C_{b^*}^2}{4\,\tilde{\epsilon}\nu_{max}}\|u_R^{j,n}-\overline{u_R^{j,n}}\|\|\nabla(u_R^{j,n}-\overline{u_R^{j,n}})\|\|\nabla u^{j,n+1}\|^2\\
&\quad+\frac{1}{4\,\tilde{\epsilon}}\frac{|\nu_j-\nu_{max}|^2}{\nu_{max}}\|\nabla\eta^{j,n}\|^2+\frac{C_{b^*}^2}{4\,\tilde{\epsilon}\,\nu_{max}}\|\nabla(\overline{u_R^{j,n}-<u_R>^n})\|^2\,\|\nabla\eta^{j,n}\|^2\\
&\quad+\frac{C_{b^*}^2}{4\,\tilde{\epsilon}\,\nu_{max}}\|\nabla(\overline{u_R^{j,n}-<u_R>^n})\|^2\,\|\nabla\eta^{j,n+1}\|^2+\frac{C_{b^*}^2\,C_{stab}}{4\,\tilde{\epsilon}\,\nu_{max}}\|\nabla\overline{u_R^{j,n}}\|\|\nabla\eta^{j,n+1}\|^2\\
&\quad+\frac{C_{b^*}^2\,C}{4\,\tilde{\epsilon}\,\nu_{max}}\|\nabla\eta^{j,n}\|^2\,. \qquad (5.28)
\end{aligned}
$$

The terms on the left hand side of (5.28) (except first) can be rearranged as follows:

$$
\begin{aligned}
&\left(\nu_{max}-\frac{13\tilde{\epsilon}}{4}\nu_{max}-\frac{|\nu_j-\nu_{max}|}{2}\right)\|\nabla\xi_R^{j,n+1}\|^2\\
&-\left(\frac{13\tilde{\epsilon}}{4}\,\nu_{max}+\frac{|\nu_j-\nu_{max}|}{2}+\frac{C_{b^*}^2\Delta t}{2}\|\|\mathbb{S}_R\|\|_2^{\frac{1}{2}}\|\nabla(\overline{u_R^{j,n}-<u_R>^n})\|^2\right)\|\nabla\xi_R^{j,n}\|^2\,. \qquad (5.29)
\end{aligned}
$$

Choosing $\tilde{\epsilon} = \frac{\epsilon}{13}$ and using (4.1) in (5.29) (5.28) yields

$$
\begin{aligned}
&\frac{1}{\Delta t}\left(\frac{1}{2}\|\xi_R^{j,n+1}\|^2 - \frac{1}{2}\|\xi_R^{j,n}\|^2\right)\\
&\quad + \left(\frac{\nu_{max}}{2} + \frac{\epsilon\,\nu_{max}}{4}\right)\left(\|\nabla\xi_R^{j,n+1}\|^2 - \|\nabla\xi_R^{j,n}\|^2\right)\\
&\quad + \nu_{max}\left(\frac{\epsilon}{2} - \frac{C_{b^*}^2\,\Delta t}{2\nu_{max}}|||\mathbb{S}_R|||_2^{\frac{1}{2}}\|\nabla(\overline{u_R^{j,n} - < u_R >^n})\|^2\right)\|\nabla\xi_R^{j,n}\|^2\\
&\leqslant \frac{13^3\,C_{b^*}^4\,C^4}{52\,\nu_{max}^3\,\epsilon^3}\|\xi_R^{j,n}\|^2 + \frac{13\,C\,\Delta t}{4\epsilon}\frac{|\nu_j - \nu_{max}|^2}{\nu_{max}} + \frac{13\,\nu_{max}}{4\epsilon}\|\nabla\eta^{j,n+1}\|^2\\
&\quad + \frac{13\,C\,C_{b^*}^2\,\Delta t}{4\,\epsilon\,\nu_{max}}\|\nabla(\overline{u_R^{j,n} - < u_R >^n})\|^2\\
&\quad + \frac{13}{4\,d\,\epsilon\,\nu_{max}}\|p^{j,n+1} - q_h^{n+1}\|^2 + \frac{13\,C\,\Delta t}{4\,\epsilon\,\nu_{max}}\\
&\quad + \frac{13\,C\,C_{b^*}^2\,\Delta t}{4\,\epsilon\nu_{max}} + \frac{13\,C_{b^*}^2}{4\,\epsilon\nu_{max}}\|u_R^{j,n} - \overline{u_R^{j,n}}\|\|\nabla(u_R^{j,n} - \overline{u_R^{j,n}})\|\|\nabla u^{j,n+1}\|^2\\
&\quad + \frac{13}{4\epsilon}\frac{|\nu_j - \nu_{max}|^2}{\nu_{max}}\|\nabla\eta^{j,n}\|^2 + \frac{13\,C_{b^*}^2}{4\,\epsilon\,\nu_{max}}\|\nabla(\overline{u_R^{j,n} - < u_R >^n})\|^2\|\nabla\eta^{j,n}\|^2\\
&\quad + \frac{13\,C_{b^*}^2}{4\,\epsilon\,\nu_{max}}\|\nabla(\overline{u_R^{j,n} - < u_R >^n})\|^2\|\nabla\eta^{j,n+1}\|^2 + \frac{13\,C_{b^*}^2\,C_{stab}}{4\,\epsilon\,\nu_{max}}\|\nabla\overline{u_R^{j,n}}\|\|\nabla\eta^{j,n+1}\|^2\\
&\quad + \frac{13\,C_{b^*}^2\,C}{4\,\epsilon\,\nu_{max}}\|\nabla\eta^{j,n}\|^2. \qquad (5.30)
\end{aligned}
$$

It follows from the stability condition (4.2) that

$$
\nu_{max}\left(\frac{\epsilon}{2} - \frac{C_{b^*}^2\,\Delta t}{2\nu_{max}}|||\mathbb{S}_R|||_2^{\frac{1}{2}}\|\nabla(\overline{u_R^{j,n} - < u_R >^n})\|^2\right) C\nu_{max}0. \qquad (5.31)
$$

Now we use (5.31), sum (5.30) from $n = 0$ to $N-1$, multiply both sides by Δt and absorb constants. Since $U_R^{j,0} = \sum_{i=1}^R (u^{j,0}, \varphi_i)\varphi_i$ we have $\|\xi_R^{j,0}\|^2 = 0$ and $\|\nabla\xi_R^{j,0}\|^2 = 0$. It then follows from (5.30)

that we have

$$\begin{aligned}
&\frac{1}{2}\|\xi_R^{j,N}\|^2 + \frac{\nu_{max}}{2}\|\nabla\xi_R^{j,N}\|^2 + \frac{\epsilon}{4}\nu_{max}\|\nabla\xi_R^{j,N}\|^2 + C\nu_{max}\Delta t\sum_{n=0}^{N-1}\|\nabla\xi_R^{j,n+1}\|^2 \\
&\leqslant \Delta t\sum_{n=0}^{N-1}\left\{\frac{C_{b^*}^4\,C^4}{\epsilon^3\,\nu_{max}^3}\|\xi_R^{j,n}\|^2 + \frac{C\Delta t}{\epsilon}\frac{|\nu_j-\nu_{max}|^2}{\nu_{max}} + \frac{C\nu_{max}}{\epsilon}\|\nabla\eta^{j,n+1}\|^2\right. \\
&\quad + \frac{C}{\epsilon}\frac{|\nu_j-\nu_{max}|^2}{\nu_{max}}\|\nabla\eta^{j,n}\|^2 + \frac{C\,C_{b^*}^2}{\epsilon\,\nu_{max}}\|\nabla(\overline{u_R^{j,n}- < u_R >^n})\|^2\|\nabla\eta^{j,n+1}\|^2 \\
&\quad + \frac{C\,C_{b^*}^2}{\epsilon\,\nu_{max}}\|\nabla(\overline{u_R^{j,n}- < u_R >^n})\|^2\|\nabla\eta^{j,n}\|^2 + \frac{C\,C_{b^*}^2\,C_{stab}}{\epsilon\,\nu_{max}}\|\nabla\overline{u_R^{j,n}}\|\|\nabla\eta^{j,n+1}\|^2 \\
&\quad \frac{C\,C_{b^*}^2}{\epsilon\nu_{max}}\|\nabla\eta^{j,n}\|^2 + \frac{C\,C_{b^*}^2\,\Delta t}{\epsilon\,\nu_{max}}\|\nabla(\overline{u_R^{j,n}- < u_R >^n})\|^2 \\
&\quad + \frac{C}{d\,\epsilon\,\nu_{max}}\|p^{j,n+1}-q_h^{n+1}\|^2 + \frac{C\,\Delta t}{\epsilon\,\nu_{max}} \\
&\quad \left. + \frac{C\,C_{b^*}^2\,\Delta t}{\epsilon\,\nu_{max}} + \frac{C\,C_{b^*}^2}{\epsilon\,\nu_{max}}\|u_R^{j,n}-\overline{u_R^{j,n}}\|\|\nabla(u_R^{j,n}-\overline{u_R^{j,n}})\|\|\nabla u^{j,n+1}\|^2\right\}. \qquad (5.32)
\end{aligned}$$

Now using Assumption 5.5, Lemma 5.8 and the stability result from Theorem 4.1, i.e., $\frac{\epsilon\,\nu_{max}\Delta t}{4}\sum_{n=0}^{N-1}\|\nabla u_R^{j,n}\|^2 \leqslant C_{stab}$, we have

$$\begin{aligned}
&\frac{\Delta t\,C\,C_{b^*}^2\,C_{stab}}{\epsilon\,\nu_{max}}\sum_{n=0}^{N-1}\|\overline{\nabla u_R^{j,n}}\|\|\nabla\eta^{j,n+1}\|^2 \\
&\leqslant \frac{\Delta t\,C\,C_{b^*}^2\,C_{stab}}{\epsilon\,\nu_{max}}\left(\sum_{n=0}^{N-1}\frac{1}{2} + \sum_{n=0}^{N-1}\frac{\|\nabla u_R^{j,n}\|^2}{2}\right) \\
&\quad \times\left((C+h^2|||\mathbb{S}_R|||_2)h^{2s} + (C+|||\mathbb{S}_R|||_2)\Delta t^4 + J_S\sum_{i=R+1}^{J_S(N_S+1)}\|\nabla\varphi_i\|^2\lambda_i\right). \qquad (5.33)
\end{aligned}$$

Rearranging the first term

$$\begin{aligned}
&\frac{\Delta t\,C\,C_{b^*}^2\,C_{stab}}{\epsilon\,\nu_{max}}\left(\sum_{n=0}^{N-1}\frac{1}{2} + \sum_{n=0}^{N-1}\frac{\|\nabla u_R^{j,n}\|^2}{2}\right) \\
&\quad = \frac{C\,C_{b^*}^2\,C_{stab}}{2\,\epsilon\,\nu_{max}} + \frac{2\,C\,C_{b^*}^2\,C_{stab}}{\epsilon^2\,\nu_{max}^2}\frac{\epsilon\nu_{max}\Delta t}{4}\left(\sum_{n=0}^{N-1}\|\nabla u_R^{j,n}\|^2\right). \qquad (5.34)
\end{aligned}$$

It then follows that

$$\frac{\Delta t\, C\, C_{b^*}^2\, C_{stab}}{\epsilon\, \nu_{max}} \sum_{n=0}^{N-1} \|\overline{\nabla u_R^{j,n}}\| \|\nabla \eta^{j,n+1}\|^2$$

$$\leqslant \left(\frac{C\, C_{b^*}^2\, C_{stab}}{2\,\epsilon\, \nu_{max}} + \frac{2\, C\, C_{b^*}^2\, C_{stab}^2}{\epsilon^2\, \nu_{max}^2} \right)$$

$$\times \left((C + h^2 |||\mathbb{S}_R|||_2) h^{2s} + (C + |||\mathbb{S}_R|||_2) \Delta t^4 + J_S \sum_{i=R+1}^{J_S(N_S+1)} \|\nabla \varphi_i\|^2 \lambda_i \right). \tag{5.35}$$

Next using Lemma 5.7 and Assumptions 2.1 and 5.6

$$\frac{C\, C_{b^*}^2\, \Delta t}{\epsilon\, \nu_{max}} \sum_{n=0}^{N-1} \|u_R^{j,n} - \overline{u_R^{j,n}}\| \|\nabla (u_R^{j,n} - \overline{u_R^{j,n}})\| \|\nabla u^{j,n+1}\|^2$$

$$\leqslant \frac{C\, C_{b^*}^2\, \Delta t}{\epsilon\, \nu_{max}} \sum_{n=0}^{N-1} \|\nabla u^{j,n+1}\|^2 \frac{1}{\delta} \left[C \left(C \left(h^{2s+2} + \Delta t^4 \right) + J_S \sum_{i=R+1}^{J_S(N_S+1)} \lambda_i \right) \right.$$

$$\left. + C\delta^2 \left((C + h^2 |||\mathbb{S}_R|||_2) h^{2s} + (C + |||\mathbb{S}_R|||_2) \Delta t^4 + J_S \sum_{i=R+1}^{J_S(N_S+1)} \|\nabla \varphi_i\|^2 \lambda_i \right) + C\delta^4 \|\Delta u_R^{j,n}\|^2 \right]$$

$$\leqslant \frac{C\, C_{b^*}^2}{\epsilon\, \nu_{max}\, \delta} \left[C \left(C \left(h^{2s+2} + \Delta t^4 \right) + J_S \sum_{i=R+1}^{J_S(N_S+1)} \lambda_i \right) \right.$$

$$\left. + C\delta^2 \left((C + h^2 |||\mathbb{S}_R|||_2) h^{2s} + (C + |||\mathbb{S}_R|||_2) \Delta t^4 + J_S \sum_{i=R+1}^{J_S(N_S+1)} \|\nabla \varphi_i\|^2 \lambda_i \right) + C\delta^4 \|\Delta u_R^{j,n}\|^2 \right]. \tag{5.36}$$

Next using theorem 4.1 we have

$$\frac{\Delta t\, C\, C_{b^*}^2}{\epsilon\, \nu_{max}} \|\nabla (\overline{u_R^{j,n} - < u_R >^n})\|^2 = \frac{C |||\mathbb{S}_R|||_2^{-\frac{1}{2}}}{\epsilon} \frac{C_{b^*}^2\, \Delta t}{\nu_{max}} |||\mathbb{S}_R|||_2^{\frac{1}{2}} \|\nabla (\overline{u_R^{j,n} - < u_R >^n})\|^2$$

$$\leqslant C |||\mathbb{S}_R|||_2^{-\frac{1}{2}}. \tag{5.37}$$

Therefore, we can bound the quantities

$$\frac{\Delta t\, C\, C_{b^*}^2}{\epsilon\, \nu_{max}} \|\nabla(\overline{u_R^{j,n} - < u_R >^n})\|^2 \|\eta_j^{n+1}\|^2 \leqslant C|||\mathbb{S}_R|||_2^{-\frac{1}{2}} \|\eta_j^{n+1}\|^2$$

$$\frac{\Delta t\, C\, C_{b^*}^2}{\epsilon\, \nu_{max}} \|\nabla(\overline{u_R^{j,n} - < u_R >^n})\|^2 \|\eta_j^{n}\|^2 \leqslant C|||\mathbb{S}_R|||_2^{-\frac{1}{2}} \|\eta_j^{n}\|^2$$

$$\frac{\Delta t^2\, C\, C_{b^*}^2}{\epsilon\, \nu_{max}} \|\nabla(\overline{u_R^{j,n} - < u_R >^n})\|^2 \leqslant C\Delta t|||\mathbb{S}_R|||_2^{-\frac{1}{2}}. \tag{5.38}$$

Now combining everything, absorbing constants, invoking the discrete Gronwall's inequality, using Assumption 5.5 and the stability estimate (4.2) (5.32) becomes

$$\begin{aligned}
&\frac{1}{2}\|\xi_R^{j,N}\|^2 + \frac{\nu_{max}}{2}\|\nabla\xi_R^{j,N}\|^2 + \frac{\epsilon}{4}\nu_{max}\|\nabla\xi_R^{j,N}\|^2 + C\nu_{max}\Delta t\sum_{n=0}^{N-1}\|\nabla\xi_R^{j,n+1}\|^2 \\
&\leqslant \exp\left(\frac{C_{b^*}^4\, C^4\, T}{\epsilon^3\, \nu_{max}^3}\right)\Bigg[\Bigg(\frac{C\,\nu_{max}\Delta t}{\epsilon} + \frac{C\Delta t}{\epsilon}\frac{|\nu_j - \nu_{max}|^2}{\nu_{max}} + 2C|||\mathbb{S}_R|||_2^{-\frac{1}{2}} + \frac{C\, C_{b^*}^2\, \Delta t}{\epsilon\, \nu_{max}} \\
&\quad + \frac{C\, C_{b^*}^2\, C_{stab}}{2\,\epsilon\,\nu_{max}} + \frac{2\,C\, C_{b^*}^2\, C_{stab}^2}{\epsilon^2\,\nu_{max}^2} + \frac{C\, C_{b^*}^2\,\delta}{\epsilon\,\nu_{max}}\Bigg) \\
&\quad \times \left((C + h^2|||\mathbb{S}_R|||_2)h^{2s} + (C + |||\mathbb{S}_R|||_2)\Delta t^4 + J_S\sum_{i=R+1}^{J_S(N_S+1)}\|\nabla\varphi_i\|^2\lambda_i\right) \\
&\quad + \frac{C\, C_{b^*}^2}{\delta\,\epsilon\,\nu_{max}}\left(C\left(h^{2s+2} + \Delta t^4\right) + J_S\sum_{i=R+1}^{J_S(N_S+1)}\lambda_i\right) + \frac{C\,\Delta t^2}{\epsilon}\frac{|\nu_j - \nu_{max}|^2}{\nu_{max}} \\
&\quad + C\Delta t|||\mathbb{S}_R|||_2^{-\frac{1}{2}} + \frac{Ch^{2s}}{d\,\epsilon\,\nu_{max}}\||p^j|\|_{2,s}^2 + \frac{C\Delta t^2}{\epsilon\,\nu_{max}} + \frac{C\, C_{b^*}^2\,\Delta t^2}{\epsilon\,\nu_{max}} + \frac{C\, C_{b^*}^2\,\delta^3}{\epsilon\,\nu_{max}}\Bigg].
\end{aligned} \tag{5.39}$$

By the triangle inequality we have $\|e^{j,n}\|^2 \leqslant 2(\|\xi_R^{j,n}\|^2 + \|\eta^{j,n}\|^2)$ from which it follows

$$\begin{aligned}
&\frac{1}{2}\|e^{j,N}\|^2 + \frac{\nu_{max}}{2}\|\nabla e^{j,N}\|^2 + \frac{\epsilon}{4}\nu_{max}\|\nabla e^{j,N}\|^2 + C\nu_{max}\Delta t\sum_{n=0}^{N-1}\|e^{j,n+1}\|^2 \\
&\quad \leqslant \|\eta^{j,N}\|^2 + \nu_{max}\|\nabla\eta^{j,N}\|^2 + \frac{\epsilon}{2}\nu_{max}\|\nabla\eta^{j,N}\|^2 + C\nu_{max}\Delta t\sum_{n=0}^{N-1}\|\eta^{j,n+1}\|^2 \\
&\qquad + \|\xi_R^{j,N}\|^2 + \nu_{max}\|\nabla\xi_R^{j,N}\|^2 + \frac{\epsilon}{2}\nu_{max}\|\nabla\xi_R^{j,N}\|^2 + C\nu_{max}\Delta t\sum_{n=0}^{N-1}\|\xi_R^{j,n+1}\|^2.
\end{aligned} \tag{5.40}$$

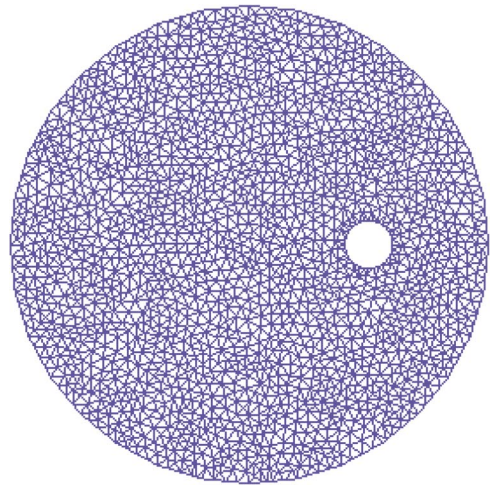

FIG. 1. Mesh for flow between offset circles resulting in 14,590 total degrees of freedom for the Taylor–Hood element pair.

Now applying inequality (5.39) and Assumption 5.5 the result follows. □

6. Numerical experiments

In this section we provide numerical experiments for the Leray ensemble-POD algorithm (3.6) demonstrating the efficacy of this approach. All computations are done using the FEniCS software suite (Logg *et al.*, 2012) and all meshes generated via the built in meshing package **mshr**.

6.1 *Problem setting*

For the numerical experiments we consider the two-dimensional flow between offset cylinders used in Gunzburger *et al.* (2017). The domain is a disk with a smaller off-center disc inside. Let $r_1 = 1$, $r_2 = 0.1$, $c_1 = 1/2$ and $c_2 = 0$; then the domain is given by

$$\Omega = \{(x, y) : x^2 + y^2 \leqslant r_1^2 \text{ and } (x - c_1)^2 + (y - c_2)^2 r_2^2\}.$$

The mesh utilized contains 14,590 degrees of freedom and is given in Fig. 1. We discretize in space via the P^2-P^1 Taylor–Hood element pair. The no-slip, no-penetration boundary conditions are imposed on both cylinders. In our test problems the flow will be driven by the counterclockwise rotational body force

$$f_{\epsilon_f}(x, y, t) = \left(-4y(1 - x^2 - y^2) + \epsilon_f sin(3\pi x)sin(3\pi y)\,,\ 4x(1 - x^2 - y^2) + \epsilon_f sin(3\pi x)sin(3\pi y)\right)^T.$$

This flow displays interesting structures that interact with the inner circle. Specifically, the flow rotates about the origin and interacts with the immersed cylinder forming a Von Kármán vortex street.

Additionally, initial conditions will be determined by solving the steady state stokes problem with the perturbed body force f_{ϵ_f}.

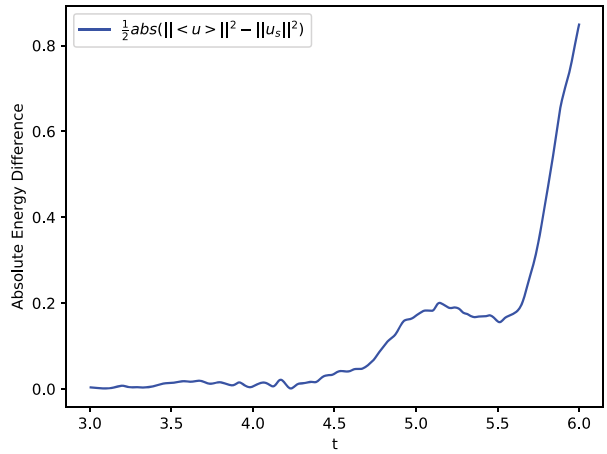

FIG. 2. The absolute difference between the kinetic energy of u_s and $< u >$.

6.2 *Experiment* 1

In this numerical example we illustrate the importance of using ensembles. Due to the nonlinearity present in the NSE, the best forecast $< u >$ is not the same as the single realization with the best data denoted by u^s. To demonstrate this we consider our test problem with two different viscosities $\nu_1 = 0.0016$ and $\nu_2 = 0.002$, and perturbations $\epsilon_{f_1} = 0.001$ $\epsilon_{f_2} = -0.001$ in the forcing term. We compare the average energy evolution of this vs. the NSE with the average of these, i.e., $\epsilon_f = 0$ and $\nu = 0.0018$. As seen in Fig. 2 there is a difference between the kinetic energy of u_s and $< u >$.

6.3 *Experiment* 2

In this experiment we demonstrate the improved accuracy and stability of the Leray ensemble-POD algorithm. In order to generate the POD basis we use two different viscosities, $\nu_1 = 0.0016$ and $\nu_2 = 0.002$. The initial conditions are generated by solving a steady Stokes problem using the previously defined counterclockwise rotational body force. We run a finite element code utilizing a linearly implicit backwards Euler method for each viscosity from $t_0 = 0$ to $T = 6$ with fixed time step $\Delta t = 0.01$. At time $T = 3.0$ we begin taking snapshots every 0.04 seconds. In Fig. 3 we show the decay of the singular values for the snapshot matrix.

To illustrate the accuracy of the Leray ensemble-POD algorithm we compare it against the ensemble-POD algorithm using the same viscosities from the offline stage. The computations are carried out over the time interval $t_0 = 3$ to $T = 6$ with fixed time step $\Delta t = 0.01$ and $r = 10$ reduced basis functions. The initial condition at $T = 3$ is the L^2 projection of the finite element solution at $T = 3.0$ into the POD space. The filtering length for the Leray ensemble-POD algorithm is taken to be $\delta = 0.025$. The filtering length is selected as the value of δ that allows the average kinetic energy of Leray ensemble-POD to most closely match the average kinetic energy of the benchmark solution (Wells *et al.*, 2017). We purposefully utilize a small number of basis functions to demonstrate the situation where the ROM does not allow for all spatial scales to be resolved. To determine the accuracy of our methods, the average of the solutions from the implicit backwards Euler method for ν_1 and ν_2 will be used as a benchmark.

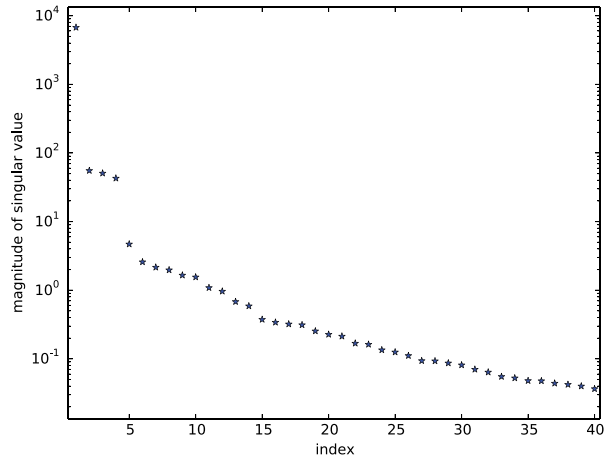

FIG. 3. The 40 largest eigenvalues for the snapshot matrix.

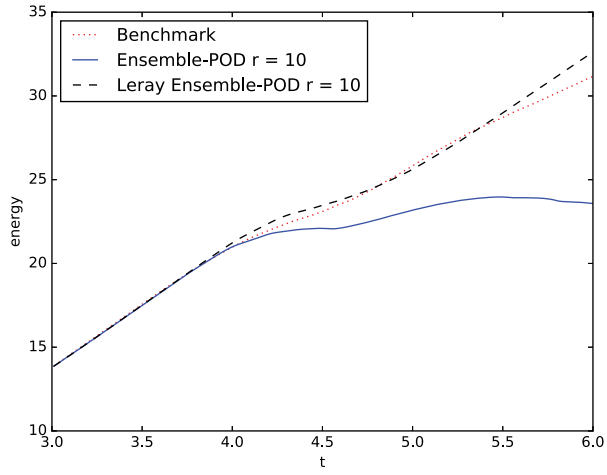

FIG. 4. For $3 \leqslant t \leqslant 6$ the average energy $\frac{1}{2}\| < u >^n \|^2$ of the Leray ensemble-POD, ensemble-POD and benchmark for Experiment 1.

In Fig. 4 we compare the average kinetic energy evolution of the Leray ensemble-POD and ensemble-POD against our benchmark solution. It can be seen that the ensemble-POD fails to match the kinetic energy of the benchmark solution, while the Leray ensemble-POD approximates it reasonably well. In Fig. 5 we compare the evolution of the error in the L^2 norm of Leray ensemble-POD and ensemble-POD algorithms. The Leray ensemble-POD has a significantly smaller error than the ensemble-POD algorithm. In Fig. 6 we plot the average POD mode evolution for ensemble-POD vs. Leray ensemble-POD. We see that, as expected, the oscillations in the POD modes are damped for Leray ensemble-POD.

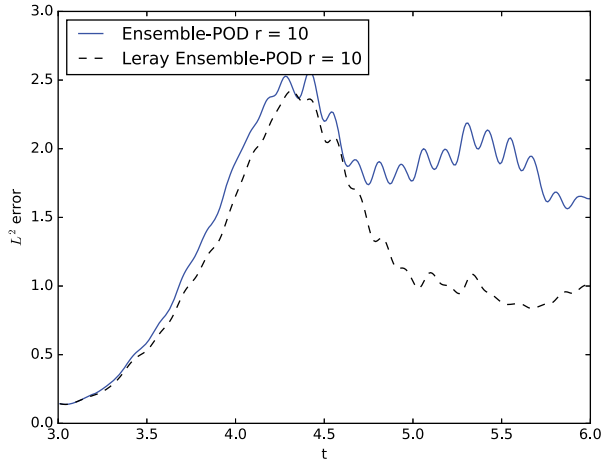

FIG. 5. For $3 \leqslant t \leqslant 6$ the L^2 error evolution of the Leray ensemble-POD and ensemble-POD algorithms with $r = 10$ basis functions.

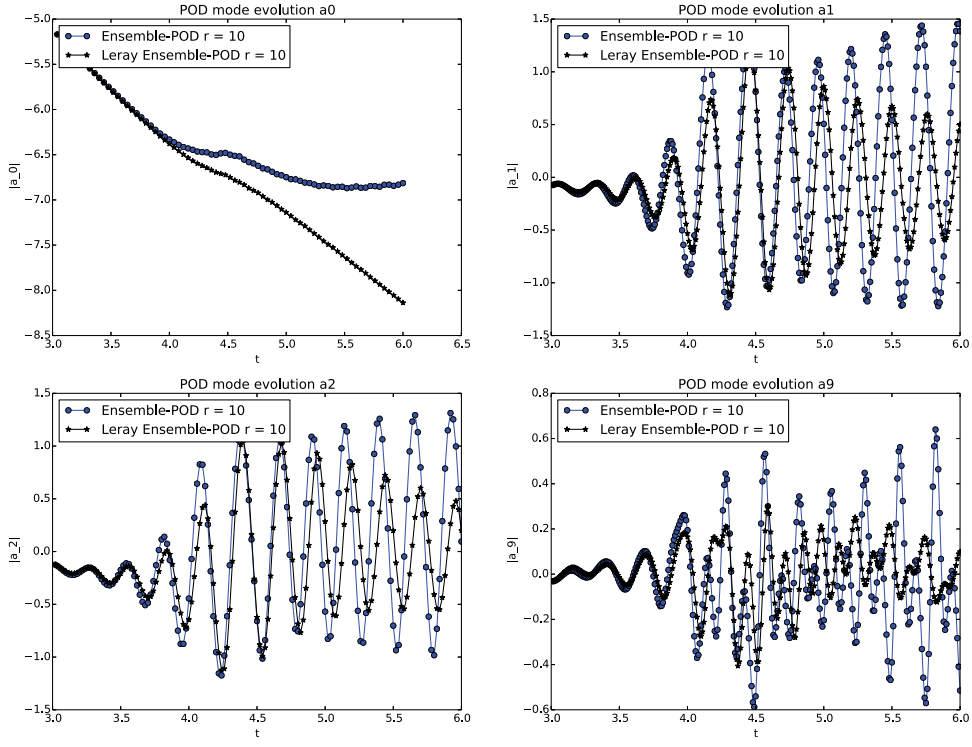

FIG. 6. The time evolution of the average POD modes for ensemble-POD vs. Leray ensemble-POD.

7. Conclusions

In this work a Leray regularized ensemble-POD method is developed for the incompressible NSEs with perturbations in the forcing function, initial conditions and viscosities. The proposed algorithm is the first ensemble-POD approach designed to work for moderate Reynolds number flows. The stability and convergence of the finite element discretization of the Leray ensemble-POD model are proven. In the numerical simulation of two-dimensional flow past two offset cylinders, it is shown that the Leray ensemble-POD model is significantly more accurate than the standard ensemble-POD model.

Acknowledgements

We thank Prof. Layton and Prof. Guermond for suggesting the use of the maximum viscosity in the new numerical discretization (2.5).

Funding

Department of Energy (DE-SC0009324 to M.G., M.S.); Air Force Office of Scientific Research (FA9550-15-1-0001 to M.G., M.S.); National Science Foundation (DMS1522656 to T.I.).

References

Anitescu, M., Pahlevani, F. & Layton, W. (2004) Implicit for local effects and explicit for nonlocal effects is unconditionally stable. *Electron. Trans. Numer. Anal.,* **18**, 174–187.

Anthony, F. J. (2018) Ensemble time-stepping algorithms for the heat equation with uncertain conductivity. *Numer. Methods Partial Differ. Equ.,* **0**, 1901–1916.

Balajewicz, M. J., Dowell, E. H. & Noack, B. R. (2013) Low-dimensional modelling of high-Reynolds-number shear flows incorporating constraints from the Navier–Stokes equation. *J. Fluid Mech.,* **729**, 285–308.

Balajewicz, M. J., Tezaur, I. & Dowell, E. H. (2016) Minimal subspace rotation on the Stiefel manifold for stabilization and enhancement of projection-based reduced order models for the compressible Navier–Stokes equations. *J. Comput. Phys.,* **321**, 224–241.

Ballarin, F., Manzoni, A., Quarteroni, A. & Rozza, G. (2015) Supremizer stabilization of POD–Galerkin approximation of parametrized steady incompressible Navier–Stokes equations. *Int. J. Numer. Methods Eng.,* **1028**, 1136–1161.

Benosman, M., Borggaard, J. & Kramer, B. (2016) Robust reduced-order model stabilization for partial differential equations based on Lyapunov theory and extremum seeking with application to the 3D Boussinesq equations. American Control Conference (ACC), 2017, pp. 1827–1832.

Carlberg, K., Farhat, C., Cortial, J. & Amsallem, D. (2013) The GNAT method for nonlinear model reduction: effective implementation and application to computational fluid dynamics and turbulent flows. *J. Comput. Phys.,* **242**, 623–647.

Chacón Rebollo, T., Delgado Ávila, E., Gómez Mármol, M., Ballarin, F. & Rozza, G. (2017) *On a certified Smagorinsky reduced basis turbulence model. SIAM J. Numer. Anal.,* **55**, 3047–3067.

Chkifa, A., Cohen, A., Migliorati, G., Nobile, F. & Tempone, R. (2015) Discrete least squares polynomial approximation with random evaluations-application to parametric and stochastic elliptic PDEs. *ESAIM Math. Model. Numer. Anal.,* **49**, 815–837.

Chkifa, A., Cohen, A. & Schwab, C. (2014) High-dimensional adaptive sparse polynomial interpolation and applications to parametric PDEs. *Found. Comput. Math.*, **14**, 601–633.

Feng, Y., Owen, D. & Perić, D. (1995) A block conjugate gradient method applied to linear systems with multiple right-hand sides. *Comput. Methods Appl. Mech. Eng.*, **127**, 203–215.

Fick, L., Maday, Y., Patera, A. T. & Taddei, T. (2017) *A reduced basis technique for long-time unsteady turbulent flows*. ArXiv e-prints.

Freund, R. W. & Malhotra, M. (1997) A block QMR algorithm for non-hermitian linear systems with multiple right-hand sides. *Linear Algebra Appl.*, **254**, 119–157.

Gallopulos, E. & Simoncini, V. (1996) Convergence of block GMRES and matrix polynomials. *Linear Algebra Appl.*, **247**, 97–119.

Ganapathysubramanian, B. & Zabaras, N. (2007) Sparse grid collocation schemes for stochastic natural convection problems. *J. Comput. Phys.*, **225**, 652–685.

Germano, M. (1986) Differential filters of elliptic type. *Phys. Fluids*, **29**, 1757–1758.

Geurts, B. J. & Holm, D. D. (2003) Regularization modeling for large-eddy simulation. *Phys. Fluids*, **15**, L13–L16.

Giere, S., Iliescu, T., John, V. & Wells, D. (2015) SUPG reduced order models for convection-dominated convection-diffusion-reaction equations. *Comput. Methods Appl. Mech. Eng.*, **289**, 454–474.

Girault, V. & Raviart, P.-A. (1979) *Finite Element Approximation of the Navier–Stokes Equations*. Lecture Notes in Mathematics, vol. 749. Berlin: Springer, p. vii+200.

Gunzburger, M. D. (2012) *Finite Element Methods for Viscous Incompressible Flows: A Guide to Theory, Practice, and Algorithms*. Boston: Elsevier.

Gunzburger, M., Jiang, N. & Schneier, M. (2017) An ensemble-proper orthogonal decomposition method for the nonstationary Navier-Stokes equations. *SIAM J. Numer. Anal.*, **55**, 286–304.

Gunzburger, M., Jiang, N. & Schneier, M. (2018) A higher-order ensemble/proper orthogonal decomposition method for the nonstationary Navier-Stokes equations. *Int. J. Numer. Anal. Model.* **15**, 608–627.

Gunzburger, M., Jiang, N. & Wang, Z. (2017a) *A second-order time-stepping scheme for simulating ensembles of parameterized flow problems*. *Computational Methods in Applied Mathematics*, to appear.

Gunzburger, M., Jiang, N. & Wang, Z. (2017b) *An efficient algorithm for simulating ensembles of parameterized flow problems*. *IMA Journal of Numerical Analysis*, dry029.

Gunzburger, M. D., Webster, C. G. & Zhang, G. (2014) Stochastic finite element methods for partial differential equations with random input data. *Acta Numer.*, **23**, 521–650.

Hesthaven, J. S., Rozza, G. & Stamm, B. (2015) *Certified Reduced Basis Methods for Parametrized Partial Differential Equations*. New York City: Springer.

Iliescu, T., Liu, H. & Xie, X. (2018) Regularized reduced order models for a stochastic Burgers equation. *Int. J. Numer. Anal. Model.* **15**, 594–607.

Iliescu, T. & Wang, Z. (2014) Variational multiscale proper orthogonal decomposition: Navier-Stokes equations. *Numer. Methods Partial Differ. Equ.*, **30**, 641–663.

Jiang, N. (2014) A higher order ensemble simulation algorithm for fluid flows. *J. Sci. Comput.*, 1–25.

Jiang, N. (2017) A second-order ensemble method based on a blended backward differentiation formula timestepping scheme for time-dependent Navier–Stokes equations. *Numer. Methods Partial Differ. Equ.*, **33**, 34–61.

Jiang, N. & Layton, W. (2014) An algorithm for fast calculation of flow ensembles. *Int. J. Uncertain. Quantif.*, **4**, 273–301.

John, V., Linke, A., Merdon, C., Neilan, M. & Rebholz, L. G. (2016) On the divergence constraint in mixed finite element methods for incompressible flows. *SIAM Rev.*, **59**, 492–544.

Johnston, H. & Liu, J.-G. (2004) Accurate, stable and efficient Navier–Stokes solvers based on explicit treatment of the pressure term. *J. Comput. Phys.*, **199**, 221–259.

Kalashnikova, I. & Barone, M. F. (2010) On the stability and convergence of a Galerkin reduced order model (ROM) of compressible flow with solid wall and far-field boundary treatment. *Int. J. Num. Meth. Eng.*, **83**, 1345–1375.

Kunisch, K. & Volkwein, S. (2001) Galerkin proper orthogonal decomposition methods for parabolic problems. *Numer. Math.*, **90**, 117–148.

Layton, W. (2008) *Introduction to the Numerical Analysis of Incompressible Viscous Flows*, vol. 6. Philadelphia: SIAM.

Layton, W., Manica, C. C., Neda, M. & Rebholz, L. G. (2008) Numerical analysis and computational testing of a high accuracy Leray-deconvolution model of turbulence. *Numer. Methods Partial Differ. Equ.*, **24**, 555–582.

Layton, W. J. & Rebholz, L. G. (2012) *Approximate Deconvolution Models of Turbulence: Analysis, Phenomenology and Numerical Analysis*, vol. 2042. Berlin, Heidelberg, New York City: Springer.

Leray, J. (1934) Sur le mouvement d'un fluide visqueux emplissant l'espace. *Acta Math.*, **63**, 193–248.

Logg, A., Mardal, K.-A. & Wells, G. (2012) *Automated Solution of Differential Equations by the Finite Element Method: The FEniCS Book*, vol. 84. New York City: Springer Science & Business Media.

Luo, Y. & Wang, Z. (2017) *An ensemble algorithm for numerical solutions to deterministic and random parabolic PDEs*. *SIAM J. Numer. Anal.,* **56**, 859–876.

Mohebujjaman, M. & Rebholz, L. G. (2017) An efficient algorithm for computation of MHD flow ensembles. *Comput. Methods Appl. Math.*, **17**, 121–137.

Nobile, F., Tempone, R. & Webster, C. G. (2008a) A sparse grid stochastic collocation method for partial differential equations with random input data. *SIAM J. Numer. Anal.*, **46**, 2309–2345.

Nobile, F., Tempone, R. & Webster, C. G. (2008b) An anisotropic sparse grid stochastic collocation method for partial differential equations with random input data. *SIAM J. Numer. Anal.*, **46**, 2411–2442.

Östh, J., Noack, B. R., Krajnović, S., Barros, D. & Borée, J. (2014) On the need for a nonlinear subscale turbulence term in POD models as exemplified for a high-Reynolds-number flow over an Ahmed body. *J. Fluid Mech.*, **747**, 518–544.

Quarteroni, A., Manzoni, A. & Negri, F. (2015) *Reduced Basis Methods for Partial Differential Equations: An Introduction*, vol. 92. New York City: Springer.

Sabetghadam, F. & Jafarpour, A. (2012) α regularization of the POD-Galerkin dynamical systems of the Kuramoto–Sivashinsky equation. *Appl. Math. Comput.*, **218**, 6012–6026.

Takhirov, A., Neda, M. & Waters, J. (2016) Time relaxation algorithm for flow ensembles. *Numer. Methods Partial Differ. Equ.*, **32**, 757–777.

Wang, Y., Navon, I. M., Wang, X. & Cheng, Y. (2016) 2D Burgers equation with large Reynolds number using POD/DEIM and calibration. *Int. J. Num. Methods Fluids*, **82**, 909–931.

Weller, J., Lombardi, E., Bergmann, M. & Iollo, A. (2009a) Numerical methods for low-order modeling of fluid flows based on POD. *Comput. Methods Appl. Mech. Eng.*, **200**, 2507–2527.

Weller, J., Lombardi, E. & Iollo, A. (2009b) Robust model identification of actuated vortex wakes. *Physica D*, **238**, 416–427.

Wells, D., Wang, Z., Xie, X. & Iliescu, T. (2017) An evolve-then-filter regularized reduced order model for convection-dominated flows. *Int. J. Num. Methods Fluids*, **84**, 598–615.

Xie, X., Mohebujjaman, M., Rebholz, L. G. & Iliescu, T. (2017a) Data-driven filtered reduced order modeling. *SIAM J. Sci. Comput,* **40**, B834–B857.

Xie, X., Wells, D., Wang, Z. & Iliescu, T. (2017b) Approximate deconvolution reduced order modeling. *Comput. Methods Appl. Mech. Eng.*, **313**, 512–534.

Xie, X., Wells, D., Wang, Z. & Iliescu, T. (2018) Numerical analysis of the Leray reduced order model. *J. Comput. Appl. Math.*, **328**, 12–29.